U.S. DEPARTMENT OF COMMERCE
NATIONAL OCEANIC AND ATMOSPHERIC ADMINISTRATION
NATIONAL WEATHER SERVICE
NATIONAL CENTERS FOR ENVIRONMENTAL PREDICTION

OFFICE NOTE 415b

AN INEXPENSIVE TECHNIQUE FOR USING PAST FORECAST ERRORS TO IMPROVE FUTURE FORECAST SKILL: PART (II) ---- A QUASI-INVERSE LINEAR METHOD

ZHAO-XIA PU
UCAR VISITING SCIENTIST PROGRAM

EUGENIA KALNAY*
ENVIRONMENTAL MODELING CENTER

MARCH 1996

**To be submitted to Monthly Weather Review
*Corresponding Author: Dr.Eugenia Kalnay, wd23ek@sun1.wwb.noaa.gov

ABSTRACT

A quasi-inverse linear method has been developed to study the sensitivity forecast errors to initial conditions for the National Centers for Environmental Prediction (NCEP)'s global spectral model. The inverse is approximated by running the tangent linear model (TLM) of the nonlinear forecast model with a negative time step, but reversing the sign of friction and diffusion terms, in order to avoid the computational instability that would be associated with these terms if they were run backwards. As usually done using the adjoint model integrations, the quasi-inverse TLM is started at the time of the verified forecast error and integrated backwards to the corresponding initial time.

First, a numerical experiment shows that this quasi-inverse linear estimation is able to trace back the differences between two perturbed forecasts from the NCEP ensemble forecasting system, and recover with good accuracy the known difference between the two forecasts at the initial time. This result shows that both the linear estimation and the quasi-inverse linear estimation are quite close to the nonlinear evolution of the perturbation in the nonlinear forecast model, suggesting that we should be able to apply the method to study of the sensitivity of forecast errors to initial conditions. We then calculate the perturbation field at the initial time (linear sensitivity perturbation) by tracing back a one-day forecast error using the TLM quasi-inverse estimation. As could be expected from the previous experiment, when the estimated error is subtracted from the original analysis, the new initial conditions lead to an almost perfect one-day forecast. The forecasts beyond day one are also considerably improved, indicating that the initial conditions have indeed been improved.

In the remainder of the paper, this quasi-inverse linear sensitivity method is compared with the adjoint sensitivity method (Pu *et al.* 1995; Rabier *et al.* 1996) for medium range weather forecasting. We find that both methods are able to trace back the forecast error to sensitivity perturbations which improve the initial conditions. However, the forecast improvement obtained by the quasi-inverse linear method is considerably better than that obtained with a single adjoint iteration, and similar to the one obtained using 5 iterations of the adjoint method, even though each adjoint iteration requires at least twice the computer resources of the quasi-inverse TLM estimation. Whereas the adjoint forecast sensitivities are closely related to singular vectors, the quasi-inverse linear sensitivities are associated with the bred (Lyapunov) vectors used for ensemble forecasting at NCEP (Toth and Kalnay 1993). The features of the two type sensitivity perturbations are also compared in this study. Finally, the possibility of the use of the sensitivity perturbation to improve future forecast skill is discussed, and preliminary experiments encourage us to further test this rather inexpensive method for possible operational use.

The model used in this study is the NCEP operational global spectral model at a resolution of T62/L28. The corresponding TLM, and its adjoint, are based on an adiabatic version of the model but include both horizontal and vertical diffusion.

1. Introduction

In the last two decades, the skill of numerical weather prediction (NWP) has improved enormously, and has become the essential guidance in most weather forecast centers. These improvements are due to three main factors: 1) the use of finer spatial resolution made possible by substantial increases in computational power and more efficient numerical techniques; 2) more comprehensive and accurate representation of the physical processes within the models; and 3) improved methods for data assimilation and use of new types of observations resulting in better initial conditions for the atmospheric models. Recent experience with data assimilation and forecast experiments suggest that large forecast errors usually arise from errors in the initial conditions rather than from errors in model formulation, at least in the extratropics (Reynolds *et al.* 1994, Simmons 1995a; Rabier *et al.* 1996;). Predictability studies such as those by Simmons *et al.* (1995b) suggest that improvements in the estimation of the initial state offer the most promising path to more accurate individual (deterministic) forecasts, although there is still scope for benefits from model improvement and from ensemble forecasting.

In recent years a considerable effort has been placed on the use of advanced data assimilation methods in order to improve the forecasts initial conditions. The 3-D variational techniques have become operationally feasible, and have been implemented in 1991 at the National Centers for Environmental Prediction (NCEP, formerly NMC) and in 1996 at the European Centre for Medium-range Weather Forecasts (ECMWF), replacing the Optimal Interpolation schemes (Derber *et al.* 1991; Parrish and Derber 1992; Andersson *et al.* 1996). The more advanced 4-D variational data assimilation method remains very expensive and still on the edge of feasibility for operational implementation (Courtier *et al.* 1994), although Zupanski and Zupanski (1996) have shown excellent convergence properties for the NCEP regional Eta model. Efforts to develop computationally feasible applications of Kalman Filtering to data assimilation are also underway (Cohn 1994). There are also studies suggesting improvement of the initial conditions by using either the forecast error itself, or the estimation of the growing modes of the atmosphere to decrease the uncertainty in the initial conditions (Kalnay and Toth 1994; Rabier *et al.* 1996).

Since it is not easy to exactly separate the errors due to the initial conditions from those due to model deficiencies, there has been a considerable interest in the investigation of the sensitivity of forecast errors to initial conditions. Recent studies with adjoint models in numerical weather prediction (Rabier *et al.* 1996; Pu *et al.* 1995) have shown that the gradient of the short-range forecast error taken with respect to the initial conditions, commonly referred

to as a "sensitivity pattern," can be an effective means of identifying structures in the initial conditions that might cause large forecast errors. Rabier *et al.* calculated a small perturbation (forecast sensitivity) in the initial conditions that minimized the observed two-day forecast error over the Northern Hemisphere using the adjoint method; the perturbation is obtained as the gradient of an error function with respect to the initial condition, multiplied by a fixed step size. Their experiments showed that the sensitivity forecasts from the adjusted (perturbed) initial conditions were better than the forecasts from the original (unperturbed) initial conditions at the same starting time (two-days old), but *not* better than the forecasts from the latest available operational initial conditions. Pu *et al.* (1995) extended this idea, by first calculating the initial perturbation of forecast sensitivity with a single iteration of conjugate-gradient method for the NCEP's global spectral forecast model, and then using the improved two-days-old initial conditions in a second iteration of the NCEP three-dimensional variational analysis cycle until the latest initial conditions are reached. Their results demonstrated that the method enhances the future medium range weather forecast skill. Since the adjoint minimization method is an iterative process, Zupanski (1995) suggested that the sensitivity pattern should also be performed iteratively. Using the NCEP regional model Eta model and its adjoint, he showed considerable improvement in the sensitivity patterns using up to 10 iterations.

In the present study we develop a quasi-inverse linear estimation of the sensitivity of forecast errors to initial conditions as an alternative to the adjoint (transpose) method used so far. The quasi-inverse is calculated by integrating the tangent linear model (TLM) backwards and thus tracing back the forecast errors to the initial time. The differences between the quasi-linear sensitivity estimation and the adjoint sensitivity pattern are then presented.

The tangent linear model (TLM) has been used in the context of sensitivity studies (Errico and Vukicevic 1992; Lacarra and Talagrand 1988; Errico *et al.* 1993), since it describes the *forward* evolution of small perturbations in a forecast model. In most cases, however, the TLM has been used to determine the evolution of small perturbations of fields in a model forecast, and, most importantly, in the development and assessment of the adjoint model. This latter application has received much attention in recently years, since the adjoint model has been extensively applied in 4-dimensional variational data assimilation (Le Dimet and Talagrand 1986; Derber 1987 and 1989; Navon *et al.* 1992; Zupanski 1993; Zou *et al.* 1992; Zupanski and Mesinger 1995) and in sensitivity analyses (Vukicevic 1991; Zou *et al.* 1992; Zupanski 1995; Pu *et al.*, 1995; Rabier *et al.* 1996). The TLM is always used to evaluate the level of accuracy of applications of its corresponding adjoint, because the accuracies of both models are strongly related, and it is usually easier to think in terms of a forward model of perturbation evolution (in

a TLM) than a backward model of sensitivities (in an adjoint). In this situation, the TLM is intended to approximately describe the evolution of the small differences between two nonlinear model solutions, where one solution begins from perturbed initial or boundary conditions, or perturbed model parameters. A TLM may be considered to be accurate as long as the solution of TLM integration from the perturbation is a good estimate of the differences between two nonlinear model integrations. There are some studies that examined the accuracy of specific TLMs in the process of creating the adjoint (transpose) model (e.g., Errico *et al.* 1993 etc.). For this reason, although the development of a TLM is not strictly necessary for many of the adjoint applications, the TLM and the adjoint are usually developed together.

So far, only the adjoint model has been used in the analysis of the sensitivity of forecast error to initial conditions, and although this application does not require the use of the TLM, it still contains the basic assumption of the TLM, namely that the error dynamics are linear. The studies of the sensitivity of forecast errors to the initial conditions have been done by defining an objective forecast error function, and trying to find a solution that minimizes this function, and therefore required the adjoint model to calculate the gradient of the function. However, in studies of the behavior of initial perturbations growing in a forecast model, there has been evidence that the TLM can be directly used to estimate the amplitude of this growing perturbation up to 1 or 2 days forecast. Lacarra and Talagrand (1988) experimentally showed that the barotropic time evolution of a small perturbation (with amplitude comparable to analysis errors) can be described by its linear approximation if the time interval is not longer than 2-3 days. Vukicevic (1991) investigated the linearity of initial error evolution using a primitive equation limited area model, and demonstrated that the major portion of initial forecast error (with magnitude comparable with analysis errors) can be described by the tangent model solutions for periods of about 1.5 days. Buizza (1994), comparing subjectively the time evolution of integrations started adding and subtracting the same structure to the control initial condition with amplitude comparable to (Optimal Interpolation) analysis error estimates, concluded that nonlinear effects are small up to forecast day 2 but they can be quite large after forecast day 4. From these experiments we can conclude that we can estimate the initial error evolution by the time integration of the TLM. If this is the case, we should consider whether we can use directly the TLM to estimate the initial error from the forecast error.

In this paper we address the following two questions: a) is it possible to estimate the initial errors from observed (perceived) short-range forecast errors through a backward integration of the TLM, and b) can we use this method to improve operational forecasts? We develop a quasi-inverse linear method to study the sensitivity forecast error to initial conditions.

The numerical experiments are performed using the NCEP operational global spectral model with full physics, with T62 (horizontal triangular truncation of 62 waves) and 28 vertical sigma levels, and the simplified corresponding TLM based on an adiabatic version (Navon *et al.* 1992) but including horizontal diffusion and vertical mixing (Pu *et al.* 1995).

The paper is organized as follows: In section 2, we describe the mathematical formulation and the projection operator used to obtain the quasi-inverse linear estimation. In section 3, the nonlinear, linear and adjoint models are described. A numerical experiment with two members of the NCEP operational forecast ensemble is performed in order to assess the accuracy of the linear forward model (propagator) and of its quasi-inverse operator. Section 4 contains numerical experiments showing the impact of the linear sensitivity (inverse of the perceived forecast error) on the forecast, and a comparison of this impact with that obtained with the adjoint sensitivity patterns. In section 5, we further compare the differences of sensitivity perturbations between the quasi-inverse TLM estimation and adjoint method. Their respective relationship to the bred (Lyapunov) and singular vectors is also discussed in Section 5. In section 6, the possibility of improving future forecast skill by using the sensitivity perturbation is tested. Section 7 is a summary and discussion.

2. Mathematical Formulation of the Quasi-Inverse Method

Consider a nonlinear forecast model M that computes the evolution of the model atmosphere from its initial state X at time t=0, to its state at time t:

$$X_t = M_t (X_0) \qquad (1)$$

The corresponding tangent linear model L propagates an perturbation of the initial state δX_0 forward in time:

$$M_t (X_0 + \delta X_0) = M_t(X_0) + L_t \delta X_0 + O(\delta X_0)^2 \qquad (2)$$

Then, given a finite initial perturbation δX_0, and its evolution through any finite time interval t, the TLM approximation can be considered reasonably accurate for as long as:

$$M_t(X_0+\delta X_0) - M_t(X_0) \approx L_t \delta X_0 \qquad (3)$$

As indicated in the introduction, for realistic atmospheric models, and for initial

perturbations with amplitudes characteristic of the estimated atmospheric analysis errors, past research experience indicates that the approximation (3) remains acceptable for about 1-3 days.

If the atmospheric model M contained only adiabatic frictionless dynamics, it would be reversible. In that case, linear tangent model would also be adiabatic and non-dissipative, and therefore reversible. A reversible model M can be easily inverted by running it backwards in time:

$$X_0 = M^{-1}(X_t) \qquad (4)$$

which is simply carried out by starting M from the "final" conditions X_t, and changing the sign of the time step Δt. The same exact inversion (running backwards in time) can be applied to a reversible TLM.

In reality, of course, comprehensive atmospheric models contain heating and frictional terms, and, like the real atmosphere, are not reversible. Nevertheless, the successful experience of early numerical weather prediction, which was based on quasigeostrophic, reversible dynamics, suggests that, at least for short range forecasts, the evolution of the atmosphere is dominated by the reversible atmospheric dynamics. In fact, the linear tangent models (and their adjoints) successfully used at the ECMWF in the development of their ensemble forecasting system contained originally only quasigeostrophic reversible dynamics (Molteni and Palmer, 1993). Later, the primitive equations were adopted for the TLM and its adjoint, again containing only reversible dynamics with the exception of a simple linear surface friction and vertical diffusion which were added *in lieu* of the full parameterization of irreversible physical processes (Buizza, 1993). This simplified adjoint was also used by Rabier *et al.* (1996) in their forecast sensitivity studies. A similar TLM with just the linearized reversible atmospheric dynamics of the NCEP global model, but including a simple linear surface friction and vertical diffusion as irreversible processes were used by Pu *et al.* (1995), and in the present work.

The dominance of the reversible dynamics in the short range forecasts, and the success of the simple TLM in describing the evolution of small perturbations, suggest that, if it was computationally feasible, backwards integration in time of the TLM would provide a fairly good approximation of its inverse, and therefore allow to trace forecast errors backwards in time and determine approximately the corresponding analysis errors. We know that dissipative terms are computationally unstable if they are integrated backwards in time, so we have a simple choice: either not to include them at all in the approximate inverse of the TLM, or, if the backward

integration without friction becomes too noisy, to include them with the sign reversed. In any case we expect the effect of these terms to be small, except perhaps near the surface.

In summary, we approximate the inverse of the TLM L_t^{-1}, by integrating the TLM backwards in time, i.e., with a negative time step, without the dissipative terms (which are small except near the surface), or by changing the sign of these terms during the backward integration. If this approximate inverse is accurate, we should be able to approximately recover the initial perturbation δX_0 from two model solutions at time t:

$$\delta X_0 \approx L_t^{-1} (M_t(X_0+\delta X_0) - M_t(X_0)) \qquad (5)$$

where L_t^{-1} represents the approximate or quasi-inverse of L_t.

Similarly, we can consider the perceived forecast error at time t given by:

$$E_t = M_t(X_0) - X_t^a \qquad (6)$$

where X_t^a is the verifying analysis valid at time t. Note that this is the perceived, and not the true error, because the verifying analysis also contains errors, but beyond 12 hours these are generally much smaller than the forecast errors. We would like to find a perturbation δX_0 that would correct the forecast:

$$M_t(X_0+\delta X_0) \approx M_t(X_0)+L_t \delta X_0 \approx X_t^a \qquad (7)$$

so that we use the approximate inverse of the TLM to obtain

$$\delta X_0 \approx L_t^{-1} (X_t^a - M_t(X_0)) \qquad (8)$$

Here δX_0 will be denoted as "sensitivity perturbation" from the quasi-inverse linear method. It is the solution obtained when we (approximately) trace the short range perceived forecast error back to the initial time. Since, as discussed above, the small dissipative terms are irreversible and we cannot invert the TLM exactly, we denote our approximation of the inverse of the TLM a "quasi-inverse". In section 3, we present numerical experiments that test the accuracy of both the linear tangent model and of its quasi-inverse for the particular model used in the present study. We have to address at least two questions: a) Is the linear evolution of the analysis error in the TLM close to the evolution of the analysis error in the nonlinear model; and

b) How accurate is the quasi-inverse linear sensitivity error , and in particular, what is the impact on the quasi-inverse of the simplified physical processes, which cannot be integrated backwards?

3. The Accuracy of The Quasi-Inverse Linear Sensitivity for NCEP Global Spectral Model

3.1 The NCEP Global Spectral Model, its TLM and Adjoint

The nonlinear atmospheric model used in this study is a lower resolution version of the operational NCEP global spectral model, with horizontal triangular truncation of T62 and 28 vertical sigma levels. This model is based on the primitive equations formulated with a spectral discretization in the horizontal and an Arakawa quadratic conserving finite differencing in the vertical (Sela 1980; Development Division staff 1988; Kanamitsu *et al.* 1991). In order to take advantage of the spectral technique in the horizontal, a vorticity and divergence representation of the momentum equations is used to eliminate the difficulties associated with the spectral representation of vector quantities on a sphere. A semi-implicit time-integration scheme is applied to the divergence, temperature, and surface pressure equations. The vorticity equations are integrated explicitly except for zonal advection which is treated implicitly. The model has a full set of physical parameterizations. New formulations of the cumulus convection and PBL parameterization were recently implemented (Pan and Wu, 1995; Hong and Pan, 1995). The model used in this study is the T62/L28 version of the T126/L28 operational model implemented in January 1995, and also used in the ensemble forecasting system, and in the NCEP/NCAR Reanalysis (Kalnay *et al.* 1996).

The tangent linear model is a simplified adiabatic version (Navon *et al.*, 1992), but it includes surface friction, horizontal diffusion and vertical mixing. With these dissipative processes the TLM was shown to represent well the evolution of small perturbations in the nonlinear model with full physics (Pu *et al.*, 1995). The full nonlinear model was used in the computation of the trajectory (basic state) used for all the linear and adjoint model integrations. The adjoint model was developed from this tangent linear model.

3.2. Test of the Accuracy of the linear and Quasi-Inverse Models

Since the analysis errors are not known, we cannot use forecast errors to test the accuracy of the quasi-inverse TLM method. Instead we chose arbitrarily two members of the operational T62 ensemble forecasting system starting from 1200 UTC 28 February 1996 (Toth and Kalnay, 1993 & 1996) for which we know exactly both the initial and the 24 hour forecast differences.

These known differences, which we can interpret as "errors", allow us to test the accuracy of the quasi-inverse of the TLM and the success of the method in correcting initial errors.

The forward TLM has been shown in Pu *et al.* (1995), in the context of an adjoint sensitivity study. They showed that the agreement between the perturbation field from the linear and nonlinear integration is good and the results indicated that the dry adiabatic linear model with surface friction and vertical diffusion can reproduce fairly well the nonlinear perturbations of the model with full physics for short range forecast.

In order to test the accuracy of the quasi-inverse TLM: the 24-hour forecast difference between the two ensemble forecast members (at 1200UTC 29 February 1996) was taken as the initial condition for the inverse integration and the TLM was integrated backwards until the corresponding initial time (1200UTC 28 February 1996) was reached, as discussed in Section 2. Fig. 1a illustrates the solution of this quasi-inverse, backward integration. It shows the linear perturbation at the initial time for the temperature, u and v wind components at sigma level 13 (about 500mb). Fig. 1b shows the corresponding exact differences between the two ensemble members at forecast initial time. The two figures are in very good agreement, indicating that the quasi-inverse method is successful in tracing back the forecast differences to the initial condition differences in this case, at least above the lower boundary layer.

We also carried out the same experiments using the TLM without the diffusive terms, but the results showed that both the forward TLM and the quasi-inverse TLM become unstable without diffusion within a one-day integration, and therefore that these terms are needed to maintain computational stability.

Finally, we then took the linear sensitivity perturbation obtained from the quasi-inverse method (as in Fig.1), and integrated it forward 24 hours with the TLM. Fig. 2a shows the obtained linear perturbation field at sigma level 13 (about 500mb), and the corresponding 24 hours fully nonlinear forecast difference is shown in Fig.2b. The agreement between the two figures is still excellent, showing that the quasi-inverse is a good approximation of the true inverse of the TLM.

We also compute an energy relative error measure of the combined quasi-inverse and TLM integration:

$$\Theta = \frac{\| LL^{-1} (M_t(X_0+\delta X_0) - M_t(X_0)) - (M_t(X_0+\delta X_0) - M_t(X_0)) \|}{\| M_t(X_0+\delta X_0) - M_t(X_0) \|} \qquad (9)$$

where the $\| \cdot \|$ denotes the kinetic energy norm(Buizza *et al.* 1993; also see (10) in section 5.1)

. Fig. 3 shows the vertical variation of the kinetic energy error ratio. There is a relatively large error in the lowest layer (almost 25%), indicating the effect of the friction term, whose sign was changed in the quasi-inverse TLM in order to maintain computational stability. For most of the atmosphere, however, the combined linear and quasi-inverse procedure is accurate to better than about 90% in the one-day sensitivity test. We also computed the errors using the total energy norm, and the relative errors were very similar to those obtained using the kinetic energy norm (Fig.3), indicating that the TLM and quasi-inverse maintain a state of quasigeostrophic balance.

4. Sensitivity of Forecast Error to Initial Conditions with Quasi-Linear Inverse Estimation

In the previous section we tested the accuracy of the linear and quasi-inverse approximations by comparing them with known differences between nonlinear integrations. In this section we test their ability to estimate errors and compare the linear and adjoint forecast sensitivity.

4.1 Quasi-Linear and adjoint forecast sensitivity

We first tested the use of the quasi-inverse TLM to obtain improved initial conditions starting from an arbitrarily chosen analysis corresponding to 0000 UTC 24 March 1995. The one-day perceived forecast error field (analysis minus forecast at 0000 UTC 25 March 1995) is used as an initial condition for the TLM backwards integration. Note that only one backward integration is needed to obtain the TLM linear initial perturbation, and that, unlike the adjoint sensitivity perturbation which provides the gradient of an error cost function, the results are not dependent on either the choice of a norm, or on the amplitude that multiplies the gradient field.

In order to compare the inverse TLM estimation with the adjoint sensitivity, we performed the experiment using the two methods for the same case. The adjoint method is used as in Pu *et al.* (1995): a sensitivity initial perturbation minimizing the norm of the one day forecast error. The minimization process is performed iteratively using a conjugate-gradient method. Note that the cost of each adjoint iteration depends on the method used to estimate the optimal step size. If the step size is fixed at a value appropriate for many different cases, as in Rabier *et al.* (1996), the cost of each adjoint iteration is equivalent to about 2 times the cost of the quasi-inverse TLM iteration. If an optimal value is determined for each case (Derber, 1987), then each iteration is about 3 times as costly as the quasi-inverse total computation. In this experiment we have followed the latter procedure.

After one iteration of the adjoint method the initial error cost function was reduced by about 20%, and after 5 iterations by about 50%. Fig. 4 shows the initial perturbation at 0000 UTC 24 March 1995 for the 500mb geopotential heights, obtained from one adjoint iteration (Fig. 4a), 5 adjoint iterations (Fig. 4b), and the quasi-inverse TLM (Fig. 4c). The amplitudes of the adjoint perturbations are considerably larger after 5 iterations than after one iteration, but even larger for the quasi-inverse TLM perturbation (note that no zero line is plotted, and a larger contour interval was used for the TLM perturbation). Close inspection of these fields reveals that there are many areas of the world where the shape of the perturbations from the 5 iterations adjoint and the inverse TLM methods is similar, although the amplitude of the latter tends to be larger (e.g., SE Australia, SE of South America, Alaska, Asia N of India, and others). On the other hand there are other areas where the shape of the 5 iterations adjoint and the inverse TLM perturbation are quite different, and even areas where the shape of the 1 and 5 iterations adjoint perturbations are also different. As will be discussed later, it is not surprising that different perturbation patterns are obtained with the two methods, because the first iteration of the adjoint method retrieves patterns corresponding only to the fastest growing singular vectors, whereas the inverse TLM method recovers both growing and decaying vectors.

To assess the quality of the three different sensitivity perturbations, i.e., the extent to which they capture the origins of the forecast errors, we performed nonlinear model integrations from the corresponding perturbed (corrected) initial conditions to 0000 UTC 25 March 1995 and compared them with the original unperturbed (control) forecast. Fig. 5 shows the one-day forecast error (difference between the forecast and analysis field, at 0000 UTC 25 March 1995) for the 500mb geopotential heights from these nonlinear model integrations starting from: a) the control analysis without corrections; and the analyses corrected with the initial errors estimated by b) the inverse TLM error estimation; c) the one-iteration adjoint sensitivity; and d) the 5-iterations adjoint sensitivity. Since all the experiments made use of the one-day forecast error of Fig. 5a, it is not surprising that they all have achieved a reduction in the one-day error, which was the original goal. It is clear from the figure that one iteration of the adjoint sensitivity method succeeds in improving the forecast error with respect to the control, and that 5 iterations are much better than a single adjoint iteration, but that the inverse TLM method gives by far the best results. A comparison of other fields (not shown) yields a similar conclusion.

Fig. 6 shows a vertical east-west vertical cross-section at 40^0 N of the height forecast error field for the control and the three improved initial conditions. It also indicates that the results from the linear sensitivity are substantially better than those of the adjoint method, even after 5 iterations. An examination of the structure of the error indicates that the quasi-inverse

linear TLM perturbation reduces very substantially the original forecast error everywhere except at a few spots near the top of the model where the TLM may have problems associated with very fast growing modes (Kalnay and Toth, 1994). The adjoint perturbations are able to reduce the forecast error in some areas, but *they actually increase significantly the original error in other areas* (e.g., near 150E a very large new error structure is introduced with the one iteration adjoint perturbation, and only partially removed by the 5 iterations perturbation). Similar results were observed for the wind forecasts (not shown). The reasons for this error may be due to the adjoint sensitivity method itself: As shown by Rabier *et al.* (1996), the first iteration in the sensitivity patterns is strongly related to the fastest growing singular vectors, each of which grows during both the backward (adjoint) and the forward integration, so that they appear with amplitudes proportional to the square of their growth rate. On the other hand, within the adjoint method, which provides the gradient of the cost function, a single optimal step size must be chosen, which Rabier *et al.* selected to optimize the reduction of error corresponding to the fastest growing singular vector. The use of a single optimal step size cannot be optimal for all the dominant singular vectors, and therefore may lead to reduction of errors for some singular vectors but to an increase for others. The adjoint sensitivity will depend on the definition of the function and minimization technique.

Since the one-day analysis is only an estimate of the true state of the atmosphere, and the perceived one-day error was used in these calculations, it is necessary to make longer forecasts to test whether the apparent improvement in the forecast error is really meaningful.

4.2 *Impact of sensitivity perturbations on medium-range forecasts*

A medium-range weather forecast was performed from each of the perturbed initial conditions discussed above. Table 1 compares the 1 through 5 days sensitivity with the control forecasts' 500mb heights anomaly correlation scores, verified against the corresponding analysis fields. We find that the sensitivity forecasts not only improve the 24-hours forecast, but also improve the rest of the 5-day forecasts. The quasi-inverse TLM estimation results in the best forecasts, although, with 5 iterations, the adjoint sensitivity is close to it, especially in the Southern Hemisphere, where analysis errors are larger, and therefore the perceived forecast error may be less reliable. The impact of the analysis errors on the perceived 24-hr forecast errors is probably the reason why the forecast improvements introduced by the TLM are equivalent to about 36 hr in the NH, and only about 12 hr in the SH. The results are similar for the 5-iterations adjoint correction, but note that each adjoint iteration requires about 2-3 times the computations required by the TLM in total.

4.3 *Improvements in original forecast quality from the sensitivity perturbation*

In order to further test the impact of TLM inverse estimation and to compare the method with adjoint approach, 14 consecutive cases from 00UTC 18 March 1995 to 00UTC 31 March 1995, were chosen for a comparison. For each case, we use the one-day forecast error at 00UTC to trace back the error in initial condition at 00UTC the day before by quasi-inverse TLM estimation and by the adjoint method. As in Rabier *et al.* (1995) and in Pu *et al.* (1995) we performed only one iteration for the adjoint method in order to minimize the computational cost. The 5-day forecasts starting from linear sensitivity initial conditions and from the sensitivity of one iteration adjoint method were compared with the original control forecast. Fig. 7a shows the anomaly correlation scores verified against the corresponding control analysis for 500mb geopotential heights in the extratropics (20° -80°), and Fig. 7b shows the root-mean-square error for 200mb and 850mb wind speed for tropical area (20^0 N - 20^0 S). The results show that in the extratropics the linear estimation method improves the original forecast in all but one case in each hemisphere, and is also better than the one iteration adjoint sensitivity forecast in all but 7 of the 28 cases. In the tropics, the adjoint forecast tends to be close to the control, because tropical perturbations tend to be slowly growing, and therefore do not dominate the adjoint perturbation (see Figs. 1-5), and the quasi-inverse TLM perturbation provides the best forecast in the majority of cases.

5. Characteristics of the different sensitivity perturbations

5.1 *Total and Kinetic Energy*

In section 3, the amplitude of the initial sensitivity perturbation from quasi-inverse TLM estimation was compared with both 1 and 5 iterations adjoint initial sensitivity perturbation for 500mb geopotential heights field. In this section, we compare the amplitude of the different initial perturbations at different vertical sigma levels. An energy norm, defined as following is used to measure the amplitude of initial perturbations:

$$E=\int_0^1\iiint_\Sigma (\nabla\Delta^{-1}\zeta\nabla\Delta^{-1}\zeta+\nabla\Delta^{-1}D\nabla\Delta^{-1}D+R_aT_r(\ln\Pi)^2+\frac{C_p}{T_r}T^2)\,d\Sigma(\frac{\partial p}{\partial z})\,d\eta \qquad (10)$$

where ζ, D, T, and Π stand for the perturbations of vorticity, divergence, temperature and surface pressure. η is the vertical coordinate, T_r is a reference temperature and R_p, C are

thermodynamic constants. Here E is the total energy norm, and the first two terms in parenthesis are the rotational and the divergent part of the kinetic energy norm.

Fig.8a shows the vertical cross section of the total energy norm and Fig. 8b the kinetic energy norm for the initial perturbation. It indicated that the magnitude of TLM sensitivity perturbation is the largest at all sigma levels. The patterns of three curves are very similar, showing the maximum amplitude at mid levels. Note that another large change of kinetic energy appears at the lowest level for the quasi-inverse TLM estimation, presumably due to the inaccuracy of the quasi-inverse at this levels, where the surface friction is most important, and its sign has been changed for computational reasons. The one-iteration adjoint does not show this effect, but the 5 iterations adjoint has also a substantial increase in both kinetic and total energy near the surface, which may be a result of the poor physics of the TLM and its adjoint.

5.2 *Fit of the perturbed initial conditions and forecasts to rawinsondes*

The RMS fit and bias of both temperature (in K) and vector winds (in m/sec) against rawinsonde data are presented in Fig. 9. In each figure, the curves on the left represent the bias, and the curves on the right the rms difference; the dashed curves indicate the fit of the control forecast, and the solid curves the fit of the perturbed forecast. Fig. 9a presents the results for the initial time, and Fig. 9b for the 24 hr forecast, for both the tropics and the NH extratropics (the results for the SH, not shown are similar to those of the NH).

In the tropics, the adjoint method introduces negligible initial differences, even after 5 iterations. The quasi-inverse linear perturbations slightly improve the bias in the temperatures and winds, but result in a significantly worst fit to the data compared to the control analysis, by about 0.1K and 1m/sec in the temperature and wind respectively. In the extratropics, a single adjoint iteration produces very small changes in the mid troposphere, and essentially no changes in the winds. After 5 iterations, the adjoint sensitivity increases by up to 0.4K the fit to the data in the lower troposphere and changes in the wind of the order of 0.5m/sec but only below 700hPa. The effect of the quasi-inverse linear sensitivity on the initial bias and rms fit in the extratropics is similar to that observed in the tropics. It should not be surprising that the perturbed initial conditions tend to fit the data worse than the control analysis, which by definition tries to optimally fit the data and the first guess.

After 24hr the perturbed forecasts are better than the control forecasts in both the tropics and the extratropics, except for the 1-iteration adjoint, which fits the winds worse than the control in the low levels of the extratropics. The improvement after 5 adjoint iterations is larger

than after one iteration, but the TLM improvement is comparable or larger. This relationship is maintained after 3 and 5 days (not shown). The improvement in the bias is also better for the quasi-inverse linear sensitivity forecast than for the adjoint forecast.

Checks of the fit of the initial conditions and forecasts against other data (aircraft reports, cloud track winds, satellite temperature soundings and surface reports) gave similar results: the linear sensitivity perturbation resulted in a fit to the data worse than the control analysis (which is designed to fit the data well), but the corresponding forecasts resulted in better fit to the data than either the control or the adjoint sensitivity forecasts.

5.3 *Sensitivity corrections and forecast error*

We now consider the evolution of the changes in the initial condition introduced by the sensitivity patterns, and how they improve the nonlinear forecast with respect to the control. This is done by measuring how parallel is the sensitivity correlation to the control error. We define as X=A(analysis)-C(control forecast) the perceived control forecast error, and Y=S (sensitivity forecast)-C is the sensitivity forecast correction. The angle between them is (e.g., Gill *et al.* 1981)

$$\alpha = \cos^{-1} \frac{(x,y)}{\|x\| \|y\|} \qquad (11)$$

where (,) denotes an inner product, and $\| \ \|$ is an Euclidian l_2-norm, in this case the total energy. If the sensitivity perturbations were able to perfectly correct the forecast, the sensitivity forecast correction would remain parallel to the control forecast error.

Fig.10 shows the variation of the angles with the forecast day. Note that at t=0, the perceived control forecast error is zero, so that the corrections cannot be compared. At 24 hour the quasi-inverse sensitivity correction is much more parallel to the control error than the adjoint 1 and 5 iteration sensitivity corrections. The advantage for the quasi-inverse method remains clear for the first two days, but then the angle increases quickly and, by day 5, it is close to the angle between the adjoint sensitivity forecast error and control error. The advantage of the quasi-inverse method may be explained by the fact that its perturbation includes all components of the error, both growing and decaying, as does the real forecast error, and therefore the correction and the error are more parallel. The adjoint sensitivity perturbations, as shown in Fig.10, on the other hand, contain only corrections in the fast growing errors, and are therefore

less parallel to the total error. After the first day or two, the growing errors dominate the total forecast error, and the advantages of the quasi-inverse linear procedure becomes less dominant. Since the quasi-inverse linear sensitivity recovers both growing and decaying errors in the initial conditions, and the adjoint sensitivity recovers only the fastest growing errors, it is not surprising that the amplitude of linear initial sensitivity perturbation is significantly larger than the adjoint sensitivity perturbation (Figs. 8 and 9).

5.4 *Sensitivity patterns, bred vectors and singular vectors*

To further interpret the different sensitivity perturbations, let us look at formula (8) again. We will show that the perturbation obtained by the quasi-inverse linear method is strongly related to the bred (Lyapunov) vectors, wheras the perturbations obtained by the one-iteration adjoint are related to the singular vectors (as shown by Rabier *et al.*, 1994). The quasi-inverse linear method attempts to find the initial perturbation δX_0 that inverts the following equation:

$$L\,\delta X_0 = \delta X_t \qquad (12)$$

where the rhs of (12) is the perceived error at time t (24 hr in our experiments):

$$\delta X_t = X_t^a - M(X_0) \qquad (13)$$

The adjoint method tries to find the initial perturbation δX_0 that maximizes the reduction of the error energy at time t, given by $\delta X_t^* \delta X_t$. From (12), we have

$$\delta X_0^* L^* L \delta X_0 = \delta X_t^* \delta X_t. \qquad (14)$$

If we expand any perturbation onto the basis formed by the singular vectors (eigenvectors of $L^* L$, with eigenvalues $\sigma_i^2 > 0$)

$$\delta X_0 = \Sigma\, \sigma_i^2\, v_i(0) \qquad (15)$$

Replacing (15) into (14), it is clear that if the error at time t is white, and projects equally onto all the singular vectors, the perturbation that will result in the maximum reduction of the rhs of (14) is the first singular vector $v_1(0)$, which grows during the interval 0-t by a factor of σ_1^2, a growth larger than that of any other perturbation. For this reason, as pointed out by Rabier *et al.* (1996), the gradient of the cost function (error energy) computed by one iteration of the

adjoint method is dominated by the leading singular vectors, and the structure of the adjoint sensitivity pattern is also very similar to that of the leading singular vectors, which are used at ECMWF as initial perturbations in their ensemble forecasting system (Molteni *et al.* 1996). When the adjoint scheme is iterated, it should eventually converge (like the quasi-inverse method) to the exact solution of (12), and, if the linearity assumption is valid, to the solution of the nonlinear error equation (4).

The quasi-inverse perturbations are also somewhat related to perturbations used for ensemble forecasting. These are the "bred" or local Lyapunov vectors used as initial perturbations in the ensemble forecast system implemented at NCEP in 1992 (Toth and Kalnay, 1993 & 1996). In the NCEP ensemble forecasting system, the breeding method used to generate perturbations simulates the development of growing errors in the analysis cycle. The perturbations are obtained as the vector difference between two nonlinear forecasts. This difference is carried forward upon the evolving atmospheric analysis field, and scaled down at regular intervals. As long as their amplitude remains small, the bred or local Lyapunov vectors generated by the difference between two nonlinear forecasts can be considered as the result of a forward integration of the TLM as in (12). Therefore, to the extent that forecast errors at time t are dominated by growing errors (leading local Lyapunov vectors), the inverse method will result in the Lyapunov vectors at time t=0. Of course, in addition to these vectors, there are decaying vectors as well in the analysis error. These decaying errors, when integrated backwards, will result in larger amplitudes at the initial time than at the final time.

6. Possible improvement of future forecast skill using sensitivity perturbations

Our results showed that the linear sensitivity patterns can improve substantially the original forecast, even beyond the period for which the error was computed (section 3). But a crucial question for the operational practice is whether we can use this procedure to improve the skill of future forecasts. For possible operational applications, we should compare the sensitivity forecast with the regular forecast from latest initial conditions. This means, in our experiments, that we should compare the 5-day sensitivity forecast scores with the 4-day forecast from the original analysis field, since the one day analysis data needed for the computation of the sensitivity perturbation introduced a one-day delay. Fig. 11 compares the anomaly correlation scores for 500mb geopotential heights, and shows that, although the 5-day sensitivity forecast is much better that the original 5-day control forecast, it is still worse than the corresponding 4-day control forecast in most cases. The same results were also obtained by using the adjoint sensitivity perturbation (Pu *et al.* 1995, Rabier *et al.* 1996). This result suggests that the latest

control forecast, based on the NCEP analysis-forecast cycle, makes better use of the data available every 6 hours, than the sensitivity forecasts which are one day longer and only use the information present in the latest analysis. However, the fact that the sensitivity 5-day forecasts are better than the original 5-day forecasts also indicates that they start from a better initial analysis than the control 5-day forecast. In order to improve the future forecast skill, Pu *et al.* (1995) suggested a technique that takes advantage of both the better starting point for the 5-day forecast provided by the sensitivity analyses, and of the use of the data in the latest day by the analysis-forecast cycle. This technique referred to as "iterated cycle" can be described as follows: a) at 0000UTC today, calculate sensitivity perturbation for initial condition at one-day-ago (t=-24 hour) from the present (today) one-day forecast error. b) Adjust the one-day-old (t=-24 hour) initial condition by using the sensitivity perturbation. c) Using this adjusted new (and presumably better) initial condition at t=-24 hour as a starting point, repeat the NCEP 3-dimensional analysis system SSI cycle every 6 hours, until the present time (0000UTC today) is reached, so that a new analysis field is obtained for today. d) Perform the medium range weather forecast from this new obtained analysis field. Following this procedure, Pu *et al.* showed that the iterated cycle with adjoint sensitivity perturbations was an improvement of the future forecast skill: the medium range forecast from the iterated cycle was better then original corresponding forecast. In a similar way, we now perform an iterated cycle by using the quasi-inverse TLM sensitivity perturbation. As can be seen from Fig.11, the new 4-day forecasts from this iterated cycle are better than the corresponding control forecasting in several cases. Fig. 12 shows the 14 cases average of forecast anomaly correlation scores which verified against the control forecast for 1-5-day forecast 500mb geopotential heights. The iterated cycle leads to a small improvement in the medium range weather forecasts, especially in Southern Hemisphere, indicating that it might be possible to use the quasi-inverse TLM sensitivity perturbation to improve future forecast skill.

7. Summary and Discussion

We have presented a quasi-inverse linear method to study the sensitivity forecast errors to initial conditions for the NCEP global spectral model. The inverse is approximated by running the tangent linear model (TLM) of the nonlinear forecast model with a negative time step, but reversing the sign of friction and diffusion terms. This avoids the computational instability that would be associated with these terms if they were run backwards. As done using the adjoint model integrations, we started the quasi-inverse TLM at the time of the verified forecast error and integrated backwards to the corresponding initial time. However, instead of minimizing an error cost function through successive iterations, as done with the adjoint sensitivity method,

the quasi-inverse linear sensitivity is obtained by a single, deterministic integration. This has the advantage that it is faster, and does not depend on the choice of the norm used in the definition of the error cost function.

A numerical experiment performed using a known perturbation from the NCEP ensemble, shows that this quasi-inverse linear estimation is able to trace back the differences between two perturbed nonlinear one-day forecasts, and recover with good accuracy the known difference between the two forecasts at the initial time. The results show that both the linear estimation and the quasi-inverse linear estimation are quite close to the nonlinear evolution of the perturbation in the nonlinear forecast model, suggesting that we should be able to apply the method to study of the sensitivity of forecast errors to initial conditions.

We then perform experiments tracing back actual forecast errors. We calculate the perturbation field at the initial time (linear sensitivity perturbation) by using perceived one-day forecast errors as initial conditions for a backward integration using the quasi-inverse TLM. As could be expected from the previous experiments, when the estimated error is subtracted from the original analysis, the new initial conditions lead to an almost perfect one-day forecast. The forecasts beyond day one are also considerably improved, indicating that the initial conditions have indeed been improved.

We then compare the quasi-inverse linear sensitivity method is with the adjoint sensitivity method (Rabier *et al.* 1996; Pu *et al.* 1995) for medium range weather forecasting. We find that although both methods are able to trace back the forecast error to sensitivity perturbations which improve the initial conditions, the forecast improvement obtained by the quasi-inverse linear method is considerably better than that obtained with a single adjoint iteration, and similar to the one obtained using 5 iterations of the adjoint method. This is true even though each adjoint iteration requires at least twice the computer resources of the inverse TLM estimation. As indicated above, the quasi-inverse TLM estimation method does not depend on the definition of a norm, it does not require the estimation of an optimal step size, and it provides an optimal correction throughout the globe.

We point out that (as shown by Rabier *et al.* 1996) that the adjoint forecast sensitivities are closely related to singular vectors. In fact, the adjoint sensitivities show several characteristics also observed in the singular vector behaviour (Szunyogh *et al.* 1996). In the initial perturbations, the wind perturbations are rather small compared to the temperature perturbations, and they are maximum at relatively low levels. After one day, however, the

maximum wind of the adjoint perturbations grow and are observed closer to the tropopause levels.

The quasi-inverse linear sensitivities are also related to ensemble perturbations, the bred (Lyapunov) vectors used for ensemble forecasting at NCEP (Toth and Kalnay 1993). If the final error is a Lyapunov vector, the inverse method will also yield an exact Lyapunov vector (except for the effect of changed sign in the dissipative terms). However, since the analysis errors contain also decaying errors, these will be magnified during the backward integration. This is one of the reasons why the quasi-inverse perturbations are much larger than those obtained with the adjoint method.

Finally, the possibility of the use of the sensitivity perturbation to improve future forecast skill is discussed, and preliminary experiments encourage us to further test this rather inexpensive method for possible operational use. Although the results are somewhat positive, this method would have to address the problem that the data is effectively used twice, and the inverse method introduces perturbations in essentially all degrees of freedom in the model, whereas the iterated analysis using adjoint perturbation method (Pu *et al.* 1995), only introduced changes into a few degrees of freedom (the leading singular vectors).

Acknowledgments

We would like to thank Dr. Zoltan Toth and Dr. O. Talagrand for helpful suggestions. Dr. Milija Zupanski provided useful suggestions for preparing the manuscript. The first author is supported by the UCAR/NCEP Visiting Scientist Program.

REFERENCES

Andersson E., P. Courtier, C. Gaffard, J. Haseler, F. Rabier, P. Unden and D.Vasiljevic, 1996: 3D-Var----the new operational analyses scheme. *ECMWF Newsletter.* Number 71-winter 1995/96. 2-5.

Buizza, R., 1994: Sensitivity of optimal unstable structures. *Q. J.Roy Meteorol. Soc.*, **120,**429-451.

Buizza, R., J. Tribbia, F. Molteni and T. Palmer, 1993: Computation of optimal unstable structure for a numerical weather prediction model. *Tellus*, **45A**, 388-407.

Cohn, S. E., N. S. Sivakumaran and R. Todling, 1994: A fixed-lag Kalman smoother for retrospective data assimilation, *Mon. Wea.Rev.*, **122**, 2838-2867.

Courtier, P., J.-N. Thepaut and A. Hollingsworth, 1994: A strategy for operational implementation of 4-D VAR using an incremental approach, *Q. J. Roy Meteorol. Soc.*, **120, 1367-1387**

Derber, J. C., 1989: A Variational continuous assimilation technique, *Mon. Wea. Rev.*, **117**, 2437-2446.

Derber, J. C.,1987: Variational four-dimensional analysis using quasi-geostrophic constraints *Mon.Wea.Rev.*, **115**. 998-1008.

Derber, J. C., D. F. Parrish, S. J. Lord, 1991: The new global operational analysis system at the national meteorological center. *Weather and Forecasting*, **6**,538-547.

Errico, R. M., T. Vukicevic, and Raeder, K., 1993: Examination of the accuracy of a tangent linear model, *Tellus*, **45A**,462-477.

Errico, R. M. and T. Vukicevic, 1992: Sensitivity analysis using an adjoint of the PSU-NCAR mesoscale model. *Mon. Wea. Rev.*, **117**,2437-2446.

Gill, P. E., W. Murray and M. H. Wright, 1981: *Practical optimization.* Academic Press, London, 401 pp.

Hong, S.-Y., and H.-L. Pan, 1995: Nonlocal boundary layer diffusion in a medium range forecast model. *Mon. Wea. Rev.*. In press.

Kalnay, E., M. Kanamitsu, R. Kistler, W. Collins *et al.*, 1996: The NCEP/NCAR 40-year reanalysis project, *Bulletin of The American Meteoro. Society*, **77**, 437-471.

Kalnay, E., and Z. Toth, 1994: Removing growing errors in the analysis. 10th conference on numerical weather prediction, July 18-22,1994,Potland, AMS, 212-215.

Kanamitsu, M., and Coauthors, 1991: Recent changes implemented into the global forecast system at NMC. *Weather & Forecasting*, **6**, 425-435.

Lacarra, J. F. and O. Talagrand, 1988: Short range evolution of small perturbation in a

barotropic model. *Tellus*, **40A**,81-95.

LeDimet, F. X., and O. Talagrand, 1986: Variational algorithms for analysis and assimilation of meteorological observations: Theoretical aspects. *Tellus*, **38A**, 91-110.

Molteni, F., R. Buizza, T. Palmer and T. Petroliagis, 1996: The ECMWF ensemble prediction system: methodology and validation. *Q.J.R. Meteorol.Soc.,**122***. 73-119.

Molteni, F., and T. N. Palmer, 1993: Predictability and finite-time instability of the northern winter circulation, *Q. J. R. Meteorol.Soc.,**121***. 269-298.

Pan, H.-L., and Wu, W.-S., 1995: Implementing a mass flux convection parameterization package for the NMC medium-range forecast model. **Office Note, 409,** NMC/NWS/NOAA, 42pp.

Parrish, D. F. and J. C. Derber, 1992: The National Meteorological Center's global spectral statistical interpolation analysis system. *Mon.Wea.Rev.*, **120**. 1747-1763.

Navon I. M., X. Zou, J. Derber and J. Sela, 1992: Variational data assimilation with an adiabatic version of the NCEP spectral model. *Mon. Wea. Rev.*, **115**,1479-1502.

Pu, Z.-X., E. Kalnay, J. C. Derber, and J. Sela, 1995: An inexpensive technique for using past forecast error to improve future forecast skill: part (I)---Adjoint method. **Office Note 415a**. National Centers for Environmental Prediction, NWS/NOAA, U. S. Department of Commerce. 46pp. (also accepted by *Q. J. Roy. Meteorol. Soc.*).

Rabier, F., E. Klinker, P. Courtier and A. Hollingsworth, 1996: Sensitivity of forecast errors to initial conditions. *Q.J.R. Meteorol.Soc.,**122***. 121-150

Reynolds, R. W., and T. M. Smith, 1994: Improved global sea surface temperature analyses using optimum interpolation. *J. Climate,* **7**, 929-948.

Sela, J. G., 1980: Spectral modeling at the National Meteorological Center. *Mon. Wea. Rev.*, **108**, 1279-1292.

Sela, J. G., H.-L. Pan *et al.* (Development Division Staff), 1988: Documentation of the research version of the NMC medium range forecasting model. (available at NCEP)

Simmons, A. J., 1995a: High-performance computing requirements for medium-range weather forecasting. *ECMWF Newsletter Number 69-Spring 1995*. 8-13.

Simmons, A. J., R. Mureau, and T. Petroliagis, 1995b: Error growth and estimates of predictability from the ECMWF forecasting system. *Q. J.Roy Meteorol. Soc.*, **121**, 1739-1771.

Szunyogh, I., E. Kalnay and Z. Toth, 1996: A comparison of lyapunov vectors and optimal vectors in a low resolution GCM. *Submitted to Tellus.*

Toth, Z., and E. Kalnay, 1996: Ensemble forecasting at NMC and the breeding method.

Submitted to *Mon.Wea.Rev.*

Toth, Z., and E. Kalnay, 1993: Ensemble forecasting at NMC: the generation of perturbations. *Bull. Amer. Meteorol. Soc.*, **74**, 2317-2330.

Vukicevic, T., 1991: Nonlinear and linear evolution of initial forecast error, *Mon.Wea.Rev.*, **119**,1602-1611

Zou, X., I.M. Navon, and F. X. LeDimet, 1992: An optimal nudging data assimilation scheme using parameter estimation. *Q.,J.,Roy.Meteorol.Soc.*, **118,** 1163-1186.

Zupanski, D. and F. Mesinger, 1995: Four-dimensional variational assimilation of precipitation data. *Mon.Wea.Rev.*, **123**. 1112-1127.

Zupanski, M., 1993: Regional four-dimensional variational data assimilation in a quasi-operational forecasting environment. *Mon.Wea.Rev.*, **121**,2396-2408

Zupanski, M., 1995, An iterative approximation to the sensitivity in calculus of variations, *Mon.Wea.Rev.*, **123**. 3590-3604.

Zupanski, M. and D. Zupanski, 1996: A quasi-operational application od a regional four-dimensional variational data assimilation. 11th Conference on Numerical Weather Prediction, Norfolk, Virginia, August 19-23, 1996. P94-95.

Figure Captions

Fig.1a the initial perturbation for temperature and wind field at sigma level 13 (about 500mb), calculated from the 24-hour forecast differences between two ensemble members by using the quasi-inverse TLM method.

Fig.1b Same as Fig.1, except the real difference between the two ensemble initial conditions.

Fig.2a 24-hour linear evolution of quasi-inverse linear sensitivity initial perturbation

Fig.2b 24-hour forecast differences between the two ensemble members.

Fig.3 The variation of the energy relative error with the vertical level.

Fig.4 Sensitivity perturbation for 500mb geopotential heights. a) from one iteration of adjoint method. b). from five iterations of adjoint method, and c) from quasi-inverse linear estimation. The contour interval is 2.5m for adjoint sensitivity but 10 m for linear sensitivity.

Fig.5 24 hours forecast geopotential heights error for 500mb from the different sensitivity initial condition. a) for control forecast; b) for quasi-inverse linear estimation. c) for one iteration adjoint; d). for 5 iterations adjoint; The forecast started from 0000UTC 24 March 1995.

Fig.6 Same as Fig.5. Except for a west-east vertical cross section at 40^0 N.

Fig.7a 5-day forecast anomaly correlation scores for 500mb geopotential heights. For control forecast (solid line), sensitivity forecast from adjoint one iteration (short dashed line) and sensitivity forecast from inverse linear estimation (long dashed line). Dates on the horizontal axis denote the starting dates of forecasts.

Fig.7b 5-day forecast Root-Mean-Square error for 850mb and 200mb wind speed. For control forecast (solid line), sensitivity forecast from adjoint one iteration (short dashed line) and sensitivity forecast from inverse linear estimation (long dashed

line). Dates on the horizontal axis denote the starting dates of forecasts.

Fig.8 The vertical cross section of the total energy norm (a) and kinetic energy norm (b) for sensitivity initial perturbation, of one iteration adjoint (solid), 5 iterations adjoint (long dashed line) and inverse linear estimation (short dashed line).

Fig.9 The Root-Mean-Square error of the sensitivity and forecast field fit the rawinsondes (observations) data. In each plot, the left two curves represent the bias, the right two curves represent the RMS error. dashed line for the control field and solid line for the sensitivity field. The vertical axis denotes the pressure. (I).Adjoint one iteration (II). Adjoint 5 iteration (III). Quasi-inverse TLM
(a). For sensitivity initial condition. **(b).** For one-day sensitivity forecast

Fig.10 The angle between forecast error and correction by sensitivity forecast. For one iteration adjoint (long dashed line), 5 iterations adjoint (short dashed line) and quasi-inverse linear estimation (solid).

Fig.11 The anomaly correlation scores for 500mb geopotential heights, for 5-day sensitivity forecast, corresponding 4-day control (operational) forecast, 5-day control forecast and for the 4-day forecast from the new cycle (iterated). Dates (March of 1995) on the horizontal axis denote the starting dates of forecasts.

Fig.12 Comparison of the average anomaly correlation scores of 1-5-day forecast for 500mb geopotential height between the iterated cycle (dashed) and control forecast (solid). Starting dates of the forecasts ranged from 18 March 1995 to 31 March 1995.

Table Captions

Table.1 Comparison of the 1-5-day forecast anomaly correlation scores for geopotential height (1-20 waves, from 0000UTC 24 March 1995)

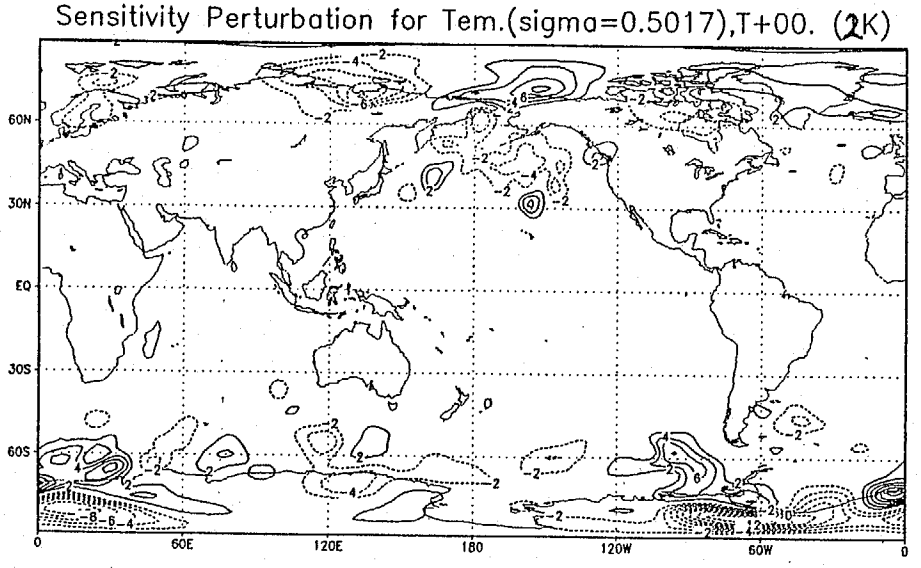
Sensitivity Perturbation for Tem.(sigma=0.5017),T+00. (2K)
60N
30N
EQ
30S
60S
0
60E
120E
180
120W
60W
0

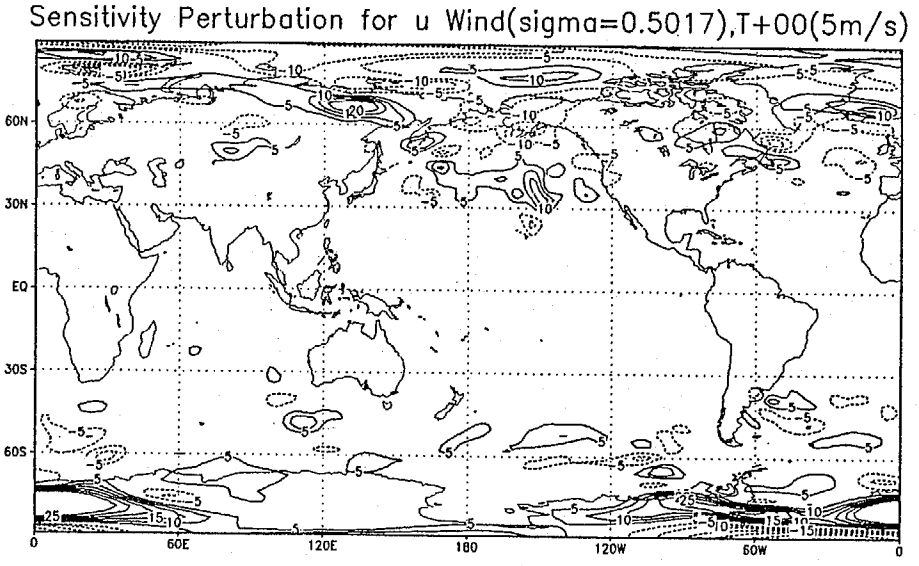
Sensitivity Perturbation for u Wind(sigma=0.5017),T+00(5m/s)
60N
30N
EQ
30S
60S
0
60E
120E
180
120W
60W
0

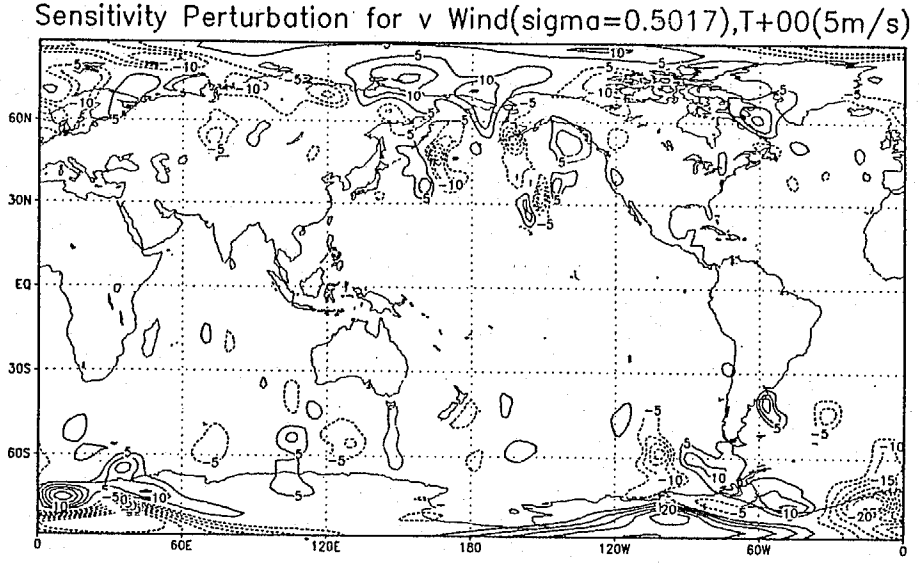
Sensitivity Perturbation for v Wind(sigma=0.5017),T+00(5m/s)
60N
30N
EQ
30S
60S
0
60E
120E
180
120W
60W
0

Fig. 1a

initial Perturbation for Tem.(sigma=0.5017),T+00. (2K)

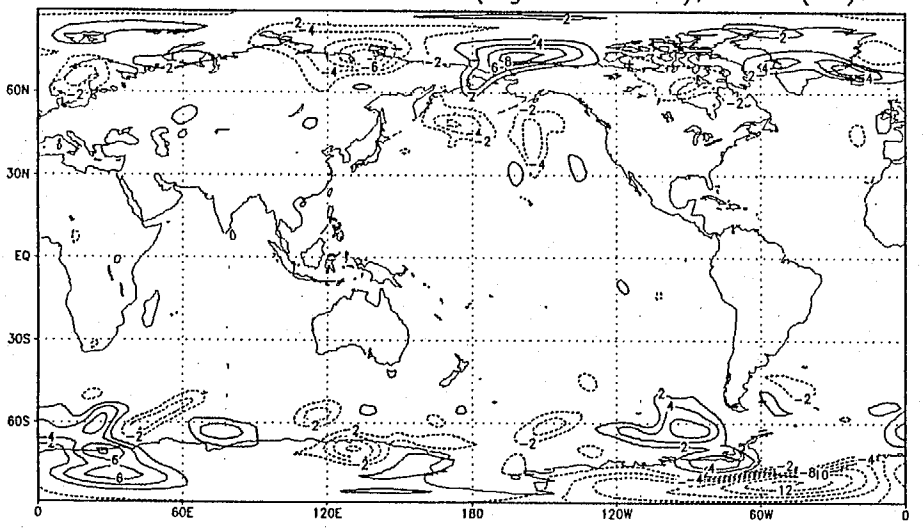

initial Perturbation for u Wind(sigma=0.5017),T+00(5m/s)

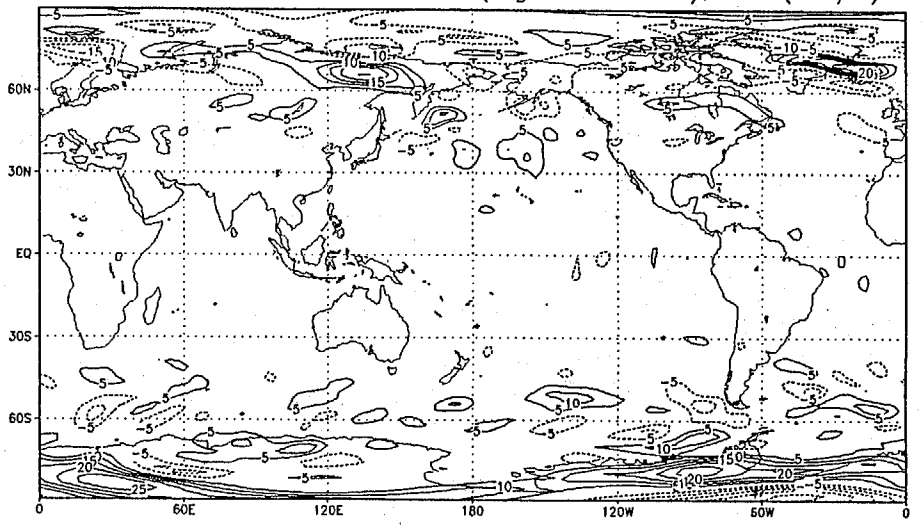

initial Perturbation for v Wind(sigma=0.5017),T+00(5m/s)

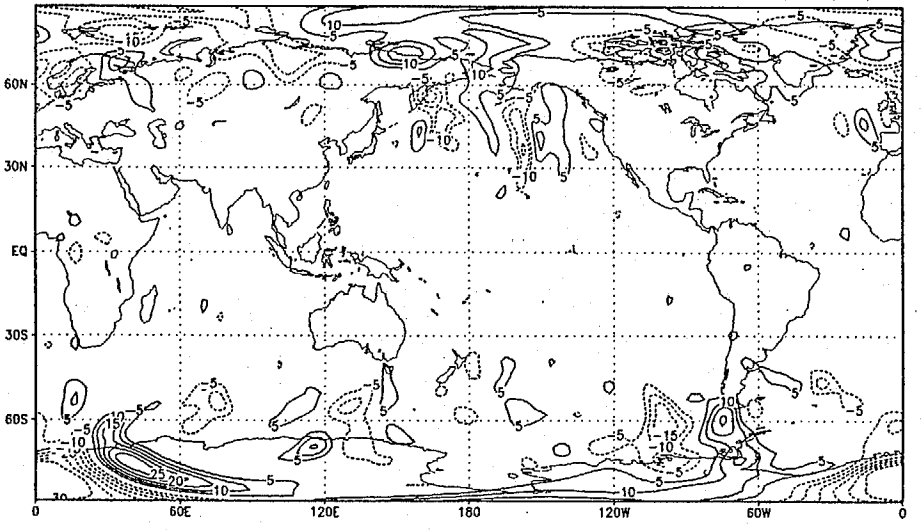

Fig. 16

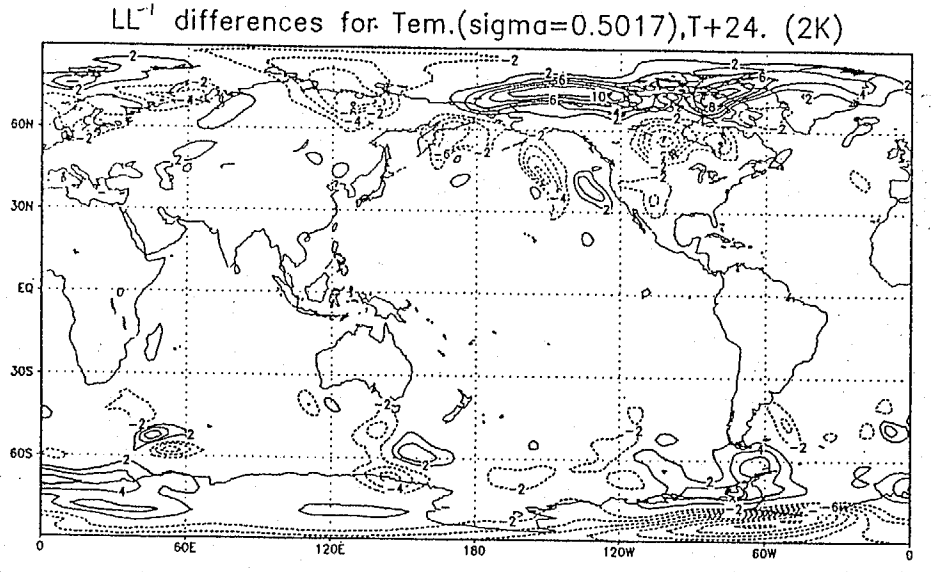
LL⁻¹ differences for Tem.(sigma=0.5017),T+24. (2K)
60N
30N
EQ
30S
60S
0
60E
120E
180
120W
60W
0

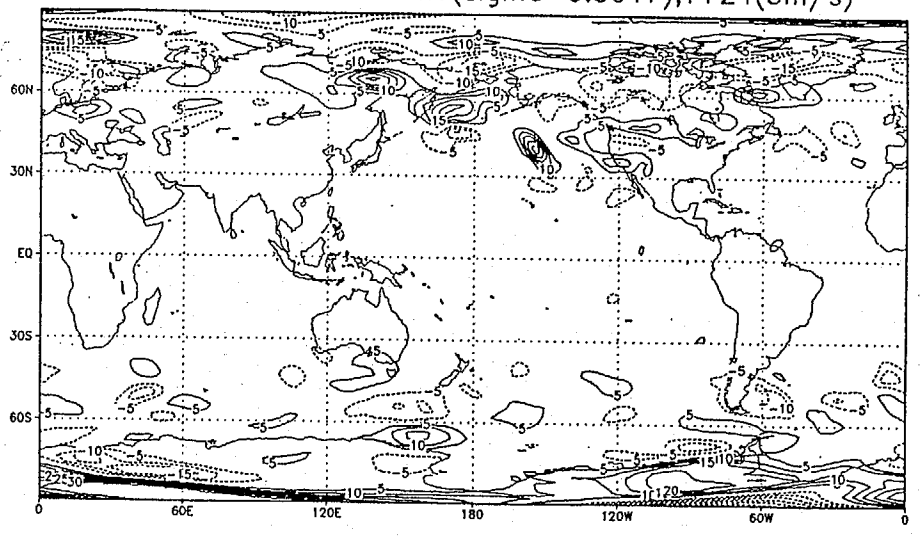
LL⁻¹ differences for u Wind(sigma=0.5017),T+24(5m/s)
60N
30N
EQ
30S
60S
0
60E
120E
180
120W
60W
0

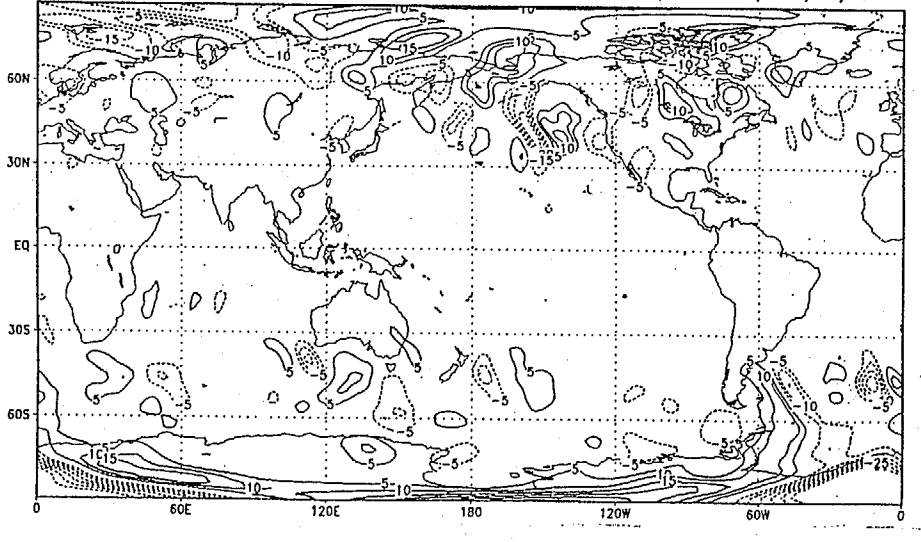
LL⁻¹ differences for v Wind(sigma=0.5017),T+24(5m/s)
60N
30N
EQ
30S
60S
0
60E
120E
180
120W
60W
0

Fig. 2a

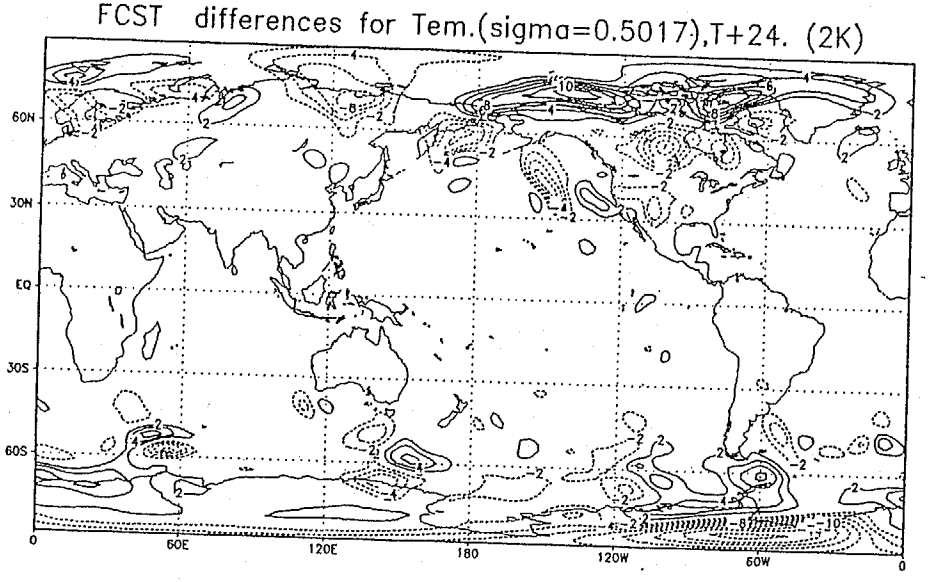
FCST differences for Tem.(sigma=0.5017),T+24. (2K)
60N
30N
EQ
30S
60S
0
60E
120E
180
120W
60W

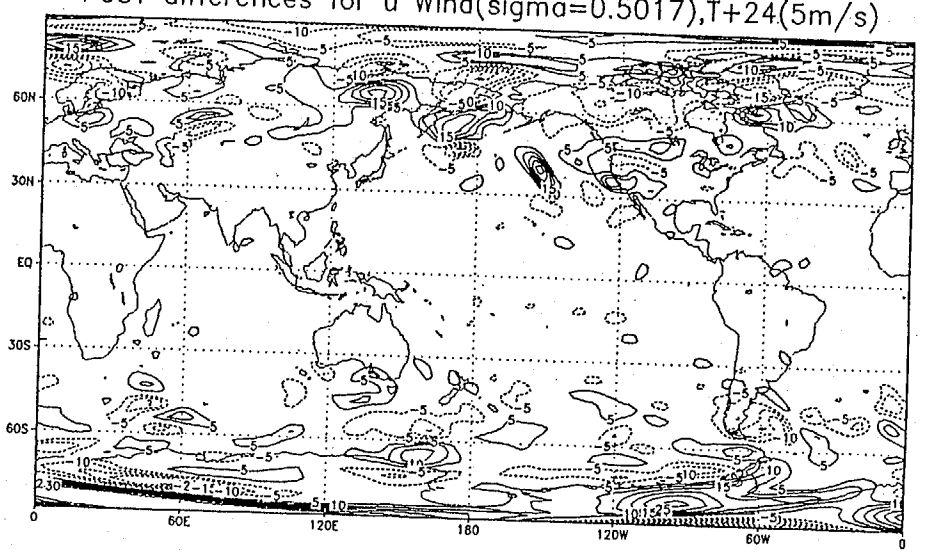
FCST differences for u Wind(sigma=0.5017),T+24(5m/s)
60N
30N
EQ
30S
60S
0
60E
120E
180
120W
60W

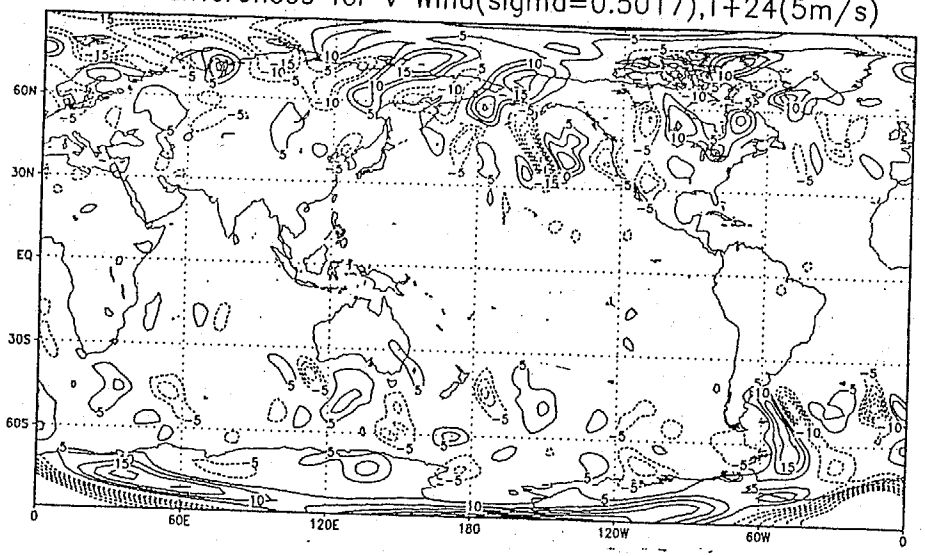
FCST differences for v Wind(sigma=0.5017),T+24(5m/s)
60N
30N
EQ
30S
60S
0
60E
120E
180
120W
60W

Fig.2b

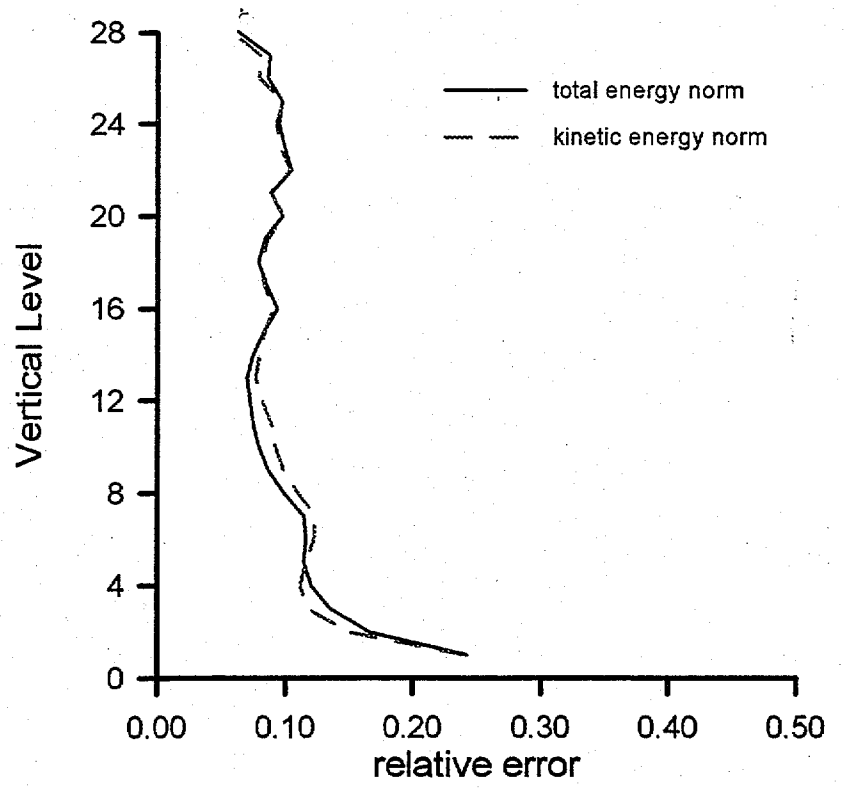
28
24
20
16
12
8
4
0
Vertical Level
0.00
0.10
0.20
0.30
0.40
0.50
relative error
total energy norm
kinetic energy norm

Fig. 3

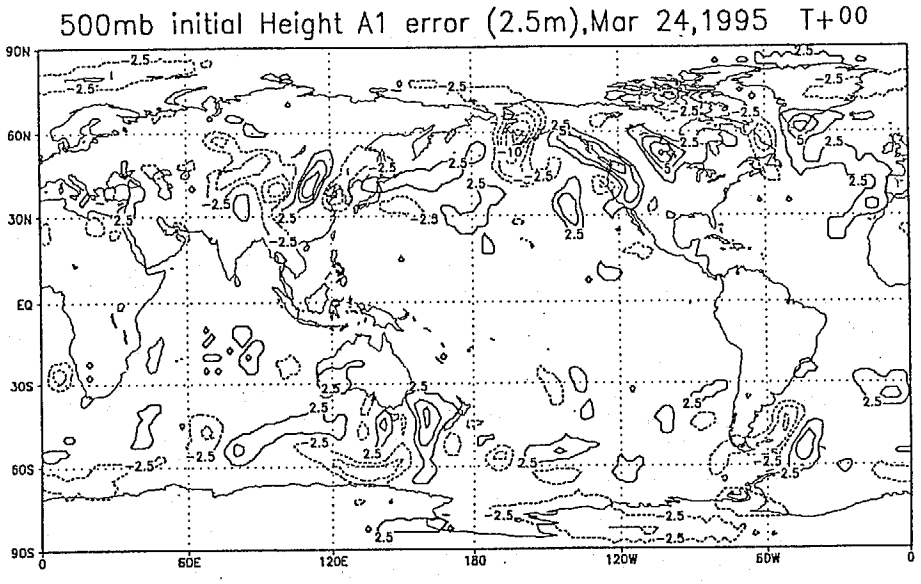
500mb initial Height A1 error (2.5m),Mar 24,1995 T+00
90N
60N
30N
EQ
30S
60S
90S
0
60E
120E
180
120W
60W
0

a

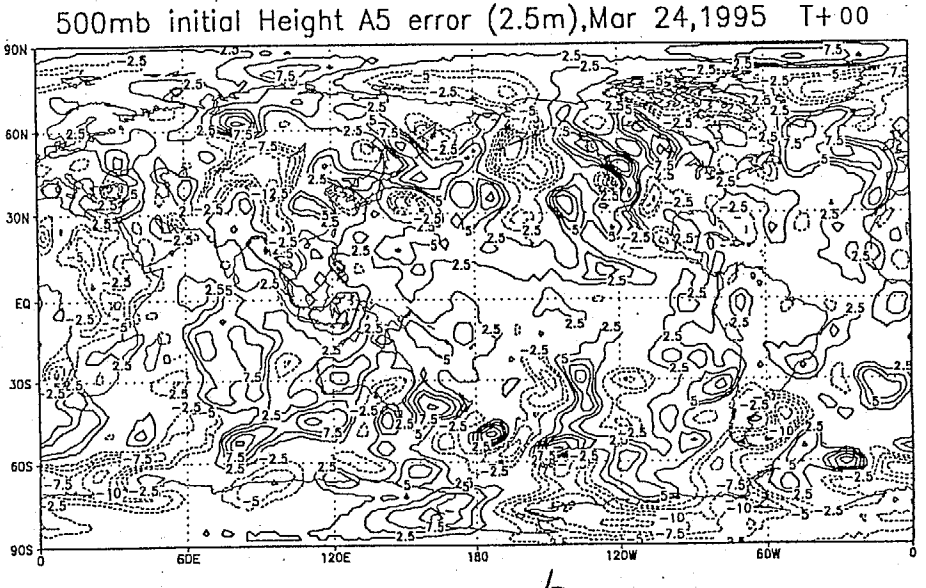
500mb initial Height A5 error (2.5m),Mar 24,1995 T+00
90N
60N
30N
EQ
30S
60S
90S
0
60E
120E
180
120W
60W
0

b

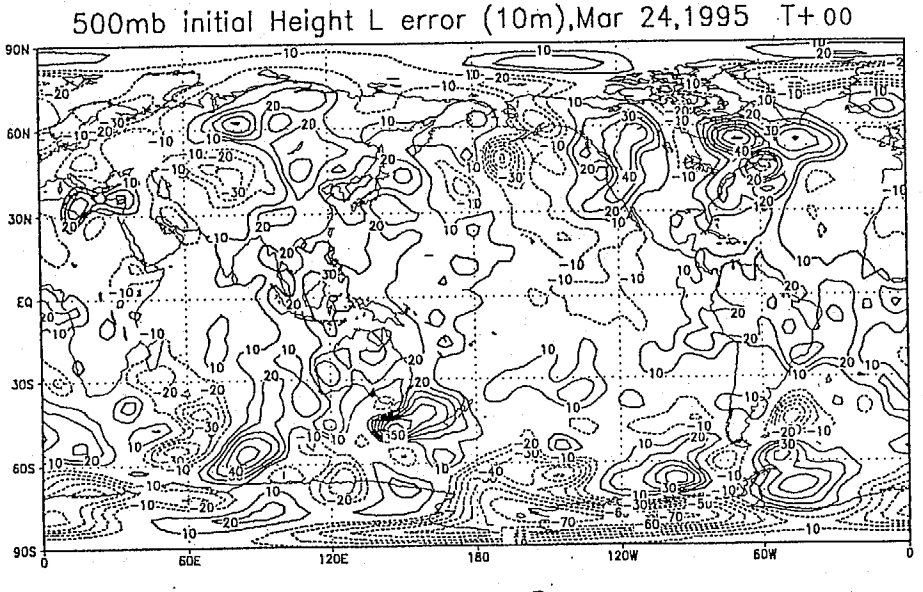
500mb initial Height L error (10m),Mar 24,1995 T+00
90N
60N
30N
EQ
30S
60S
90S
0
60E
120E
180
120W
60W
0

c

Fig. 4

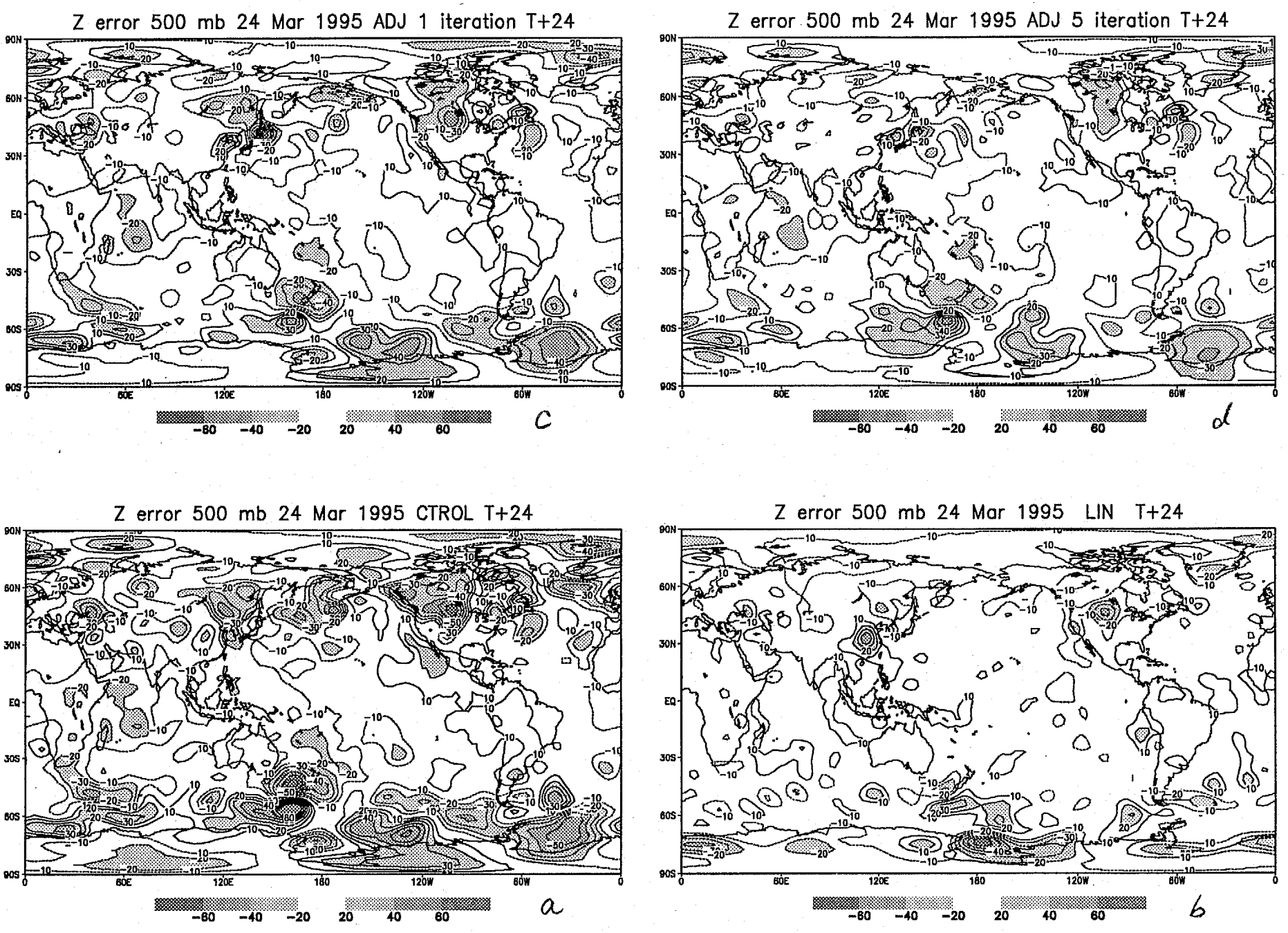
Z error 500 mb 24 Mar 1995 ADJ 1 iteration T+24
Z error 500 mb 24 Mar 1995 ADJ 5 iteration T+24
Z error 500 mb 24 Mar 1995 CTROL T+24
Z error 500 mb 24 Mar 1995 LIN T+24
90N
60N
30N
EQ
30S
60S
90S
0
60E
120E
180
120W
60W
-80 -40 -20 20 40 60
c
d
a
b

Fig. 5

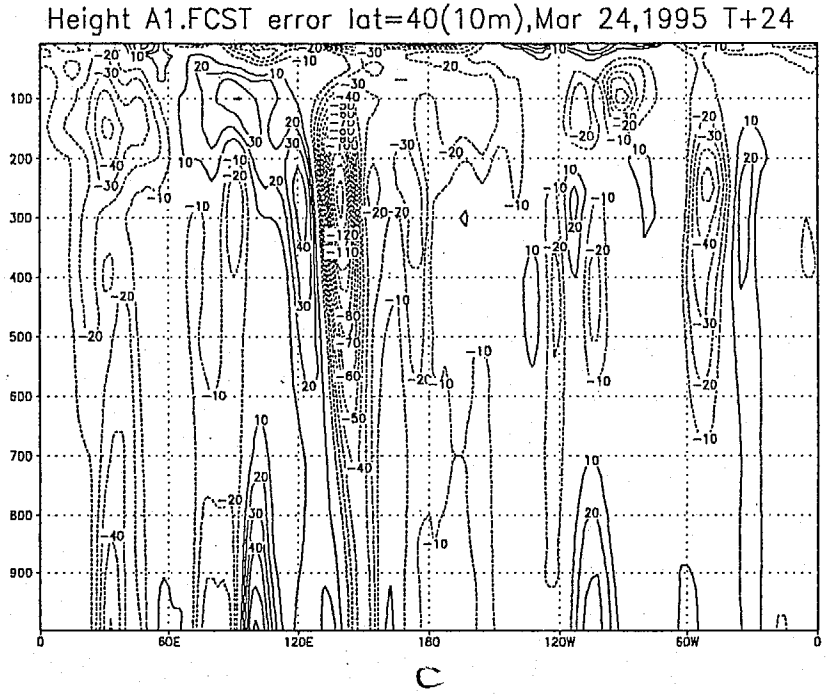
Height A1.FCST error lat=40(10m),Mar 24,1995 T+24
100
200
300
400
500
600
700
800
900
0
60E
120E
180
120W
60W
0

c

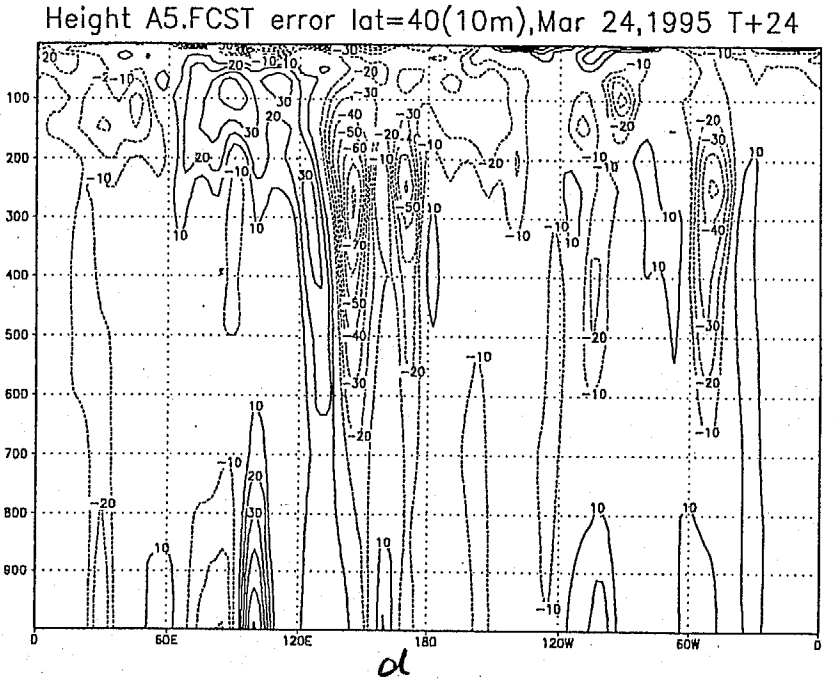
Height A5.FCST error lat=40(10m),Mar 24,1995 T+24
100
200
300
400
500
600
700
800
900
0
60E
120E
180
120W
60W
0

d

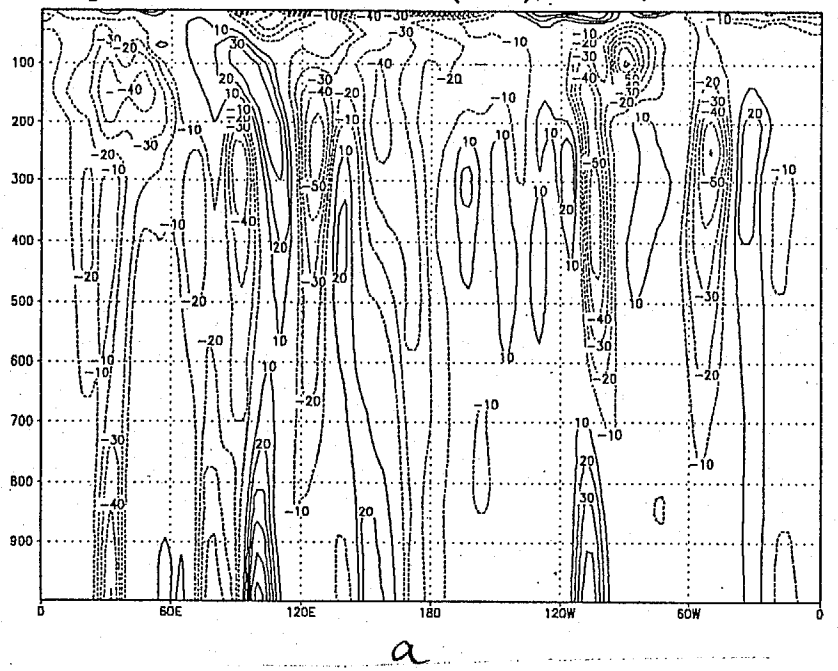
Height ctrl.FCST error lat=40(10m),Mar 24,1995 T+24
100
200
300
400
500
600
700
800
900
0
60E
120E
180
120W
60W
0

a

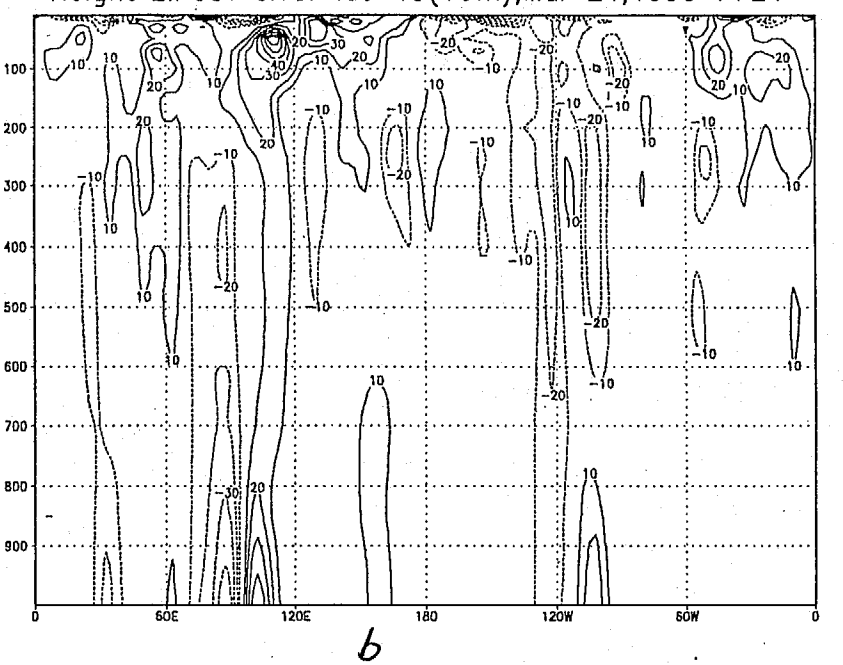
Height L.FCST error lat=40(10m),Mar 24,1995 T+24
100
200
300
400
500
600
700
800
900
0
60E
120E
180
120W
60W
0

b

Fig. 6

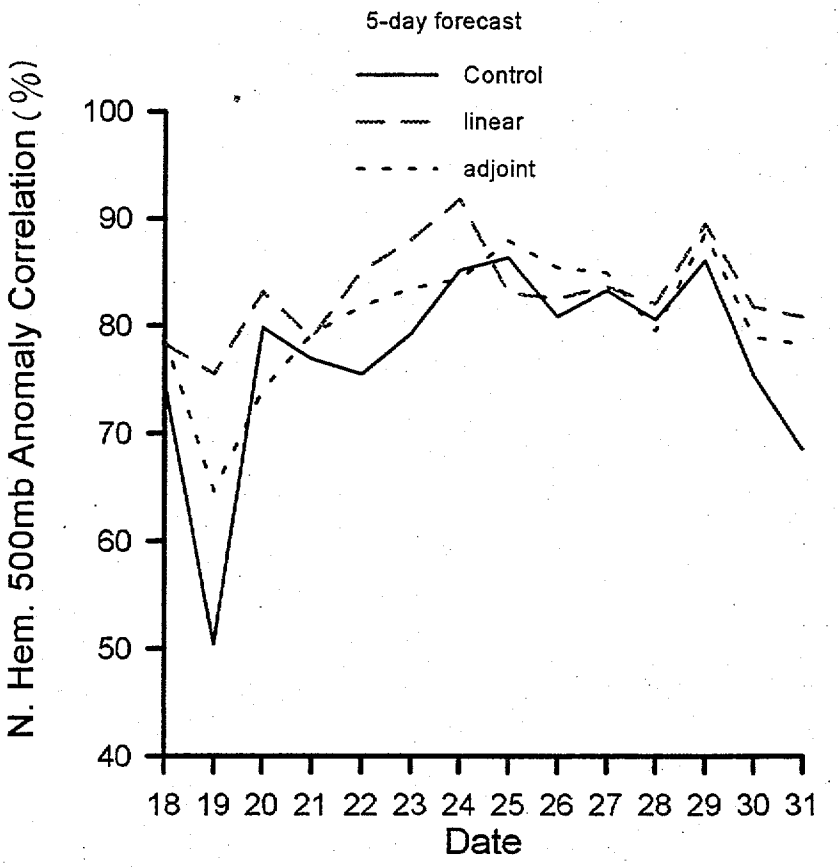
5-day forecast
Control
linear
adjoint
N. Hem. 500mb Anomaly Correlation (%)
100
90
80
70
60
50
40
18 19 20 21 22 23 24 25 26 27 28 29 30 31
Date

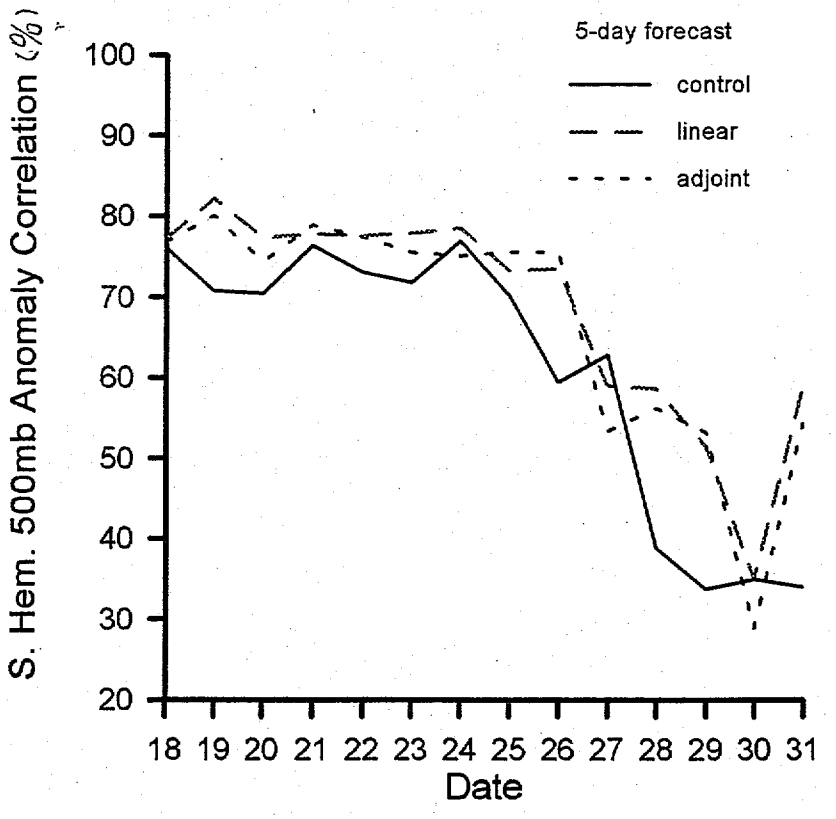
5-day forecast
control
linear
adjoint
S. Hem. 500mb Anomaly Correlation (%)
100
90
80
70
60
50
40
30
20
18 19 20 21 22 23 24 25 26 27 28 29 30 31
Date

Fig. 7a

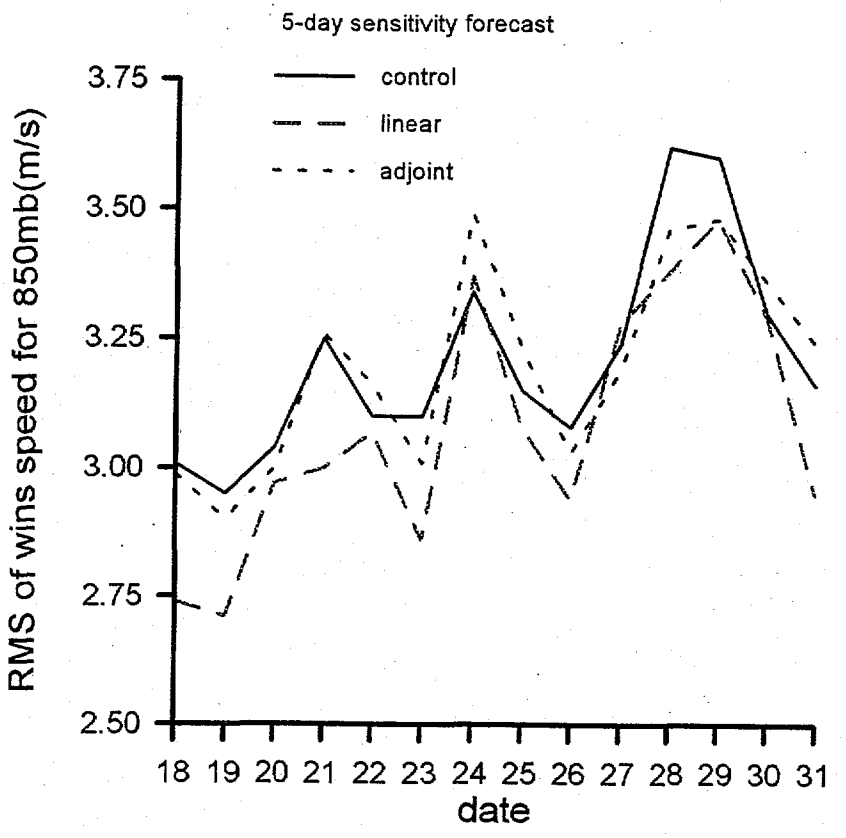
5-day sensitivity forecast
control
linear
adjoint
RMS of wins speed for 850mb(m/s)
3.75
3.50
3.25
3.00
2.75
2.50
18 19 20 21 22 23 24 25 26 27 28 29 30 31
date

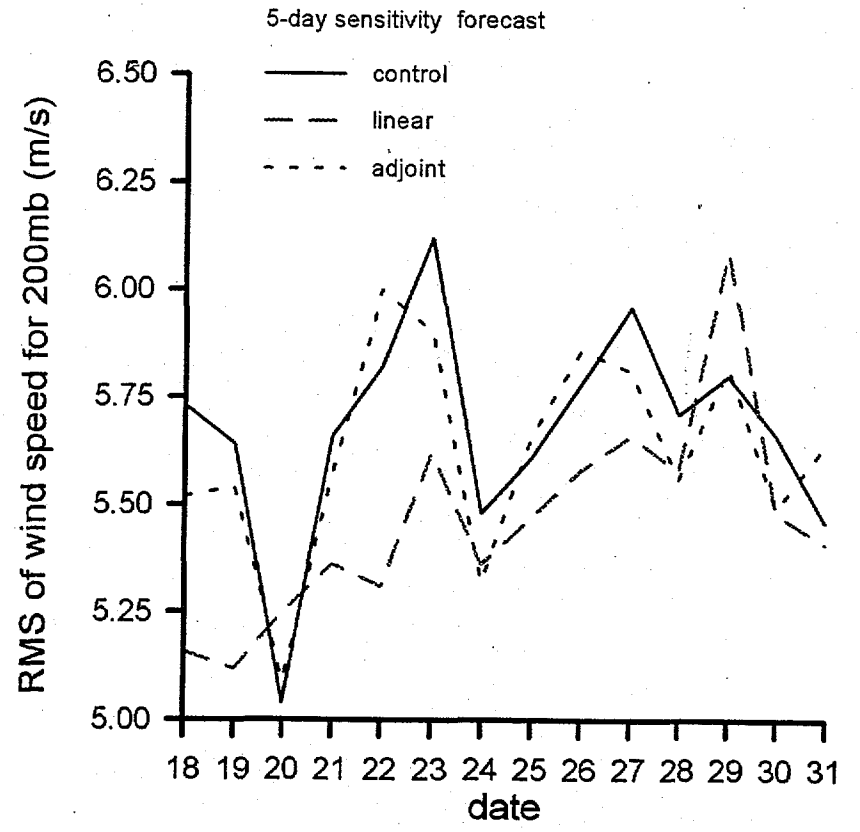
5-day sensitivity forecast
control
linear
adjoint
RMS of wind speed for 200mb (m/s)
6.50
6.25
6.00
5.75
5.50
5.25
5.00
18 19 20 21 22 23 24 25 26 27 28 29 30 31
date

Fig. 7b

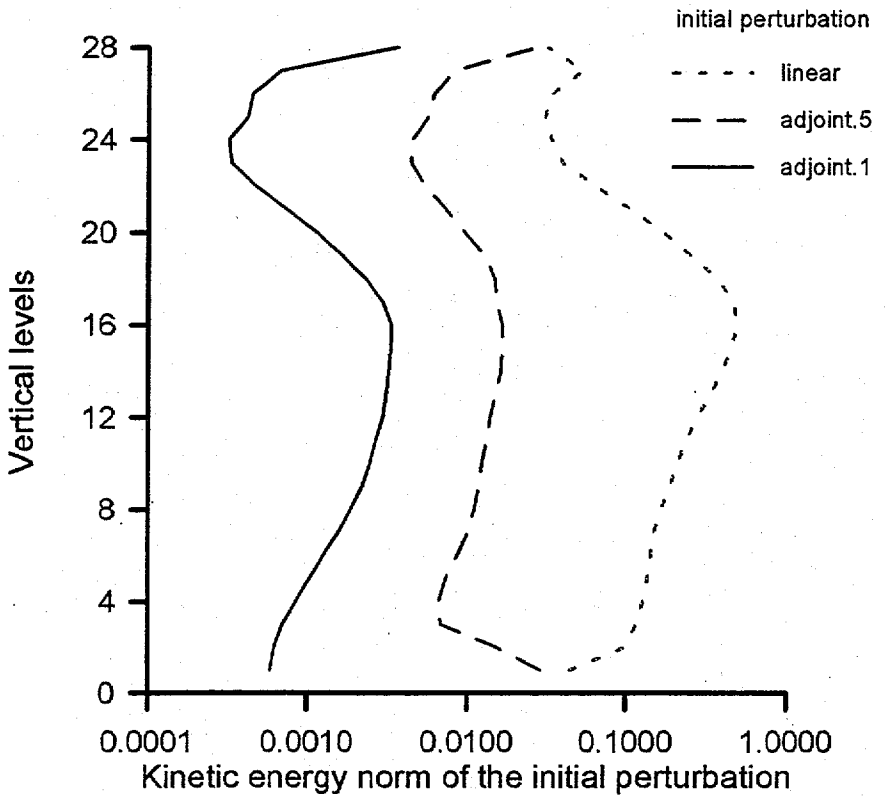
initial perturbation
linear
adjoint.5
adjoint.1
Vertical levels
28
24
20
16
12
8
4
0
0.0001
0.0010
0.0100
0.1000
1.0000
Kinetic energy norm of the initial perturbation

Fig. 8b

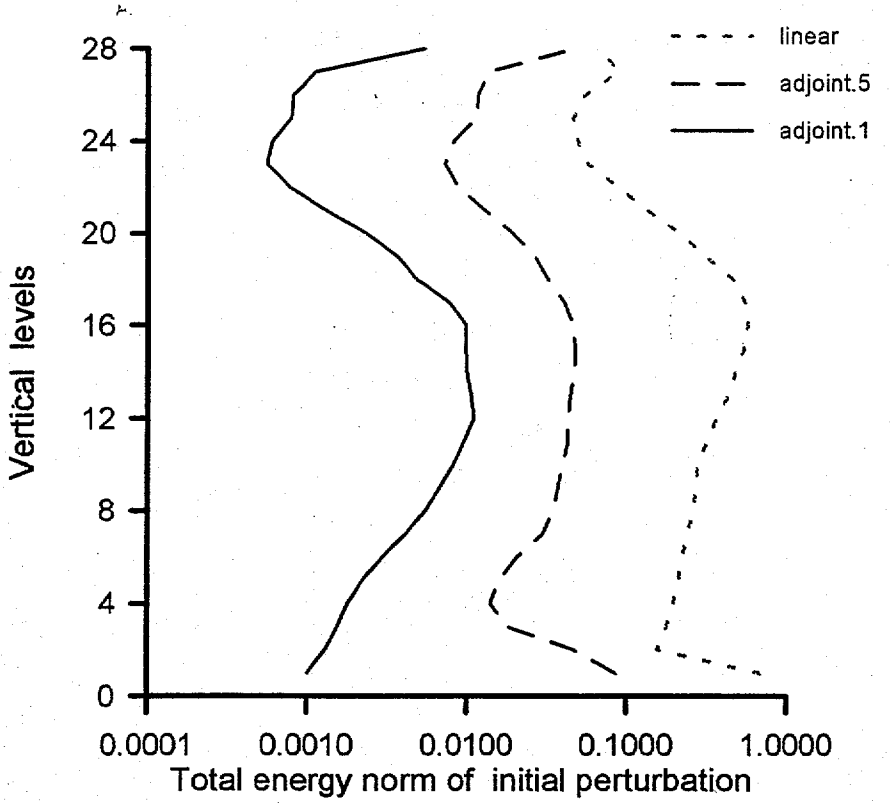
linear
adjoint.5
adjoint.1
Vertical levels
28
24
20
16
12
8
4
0
0.0001
0.0010
0.0100
0.1000
1.0000
Total energy norm of initial perturbation

Fig. 8a

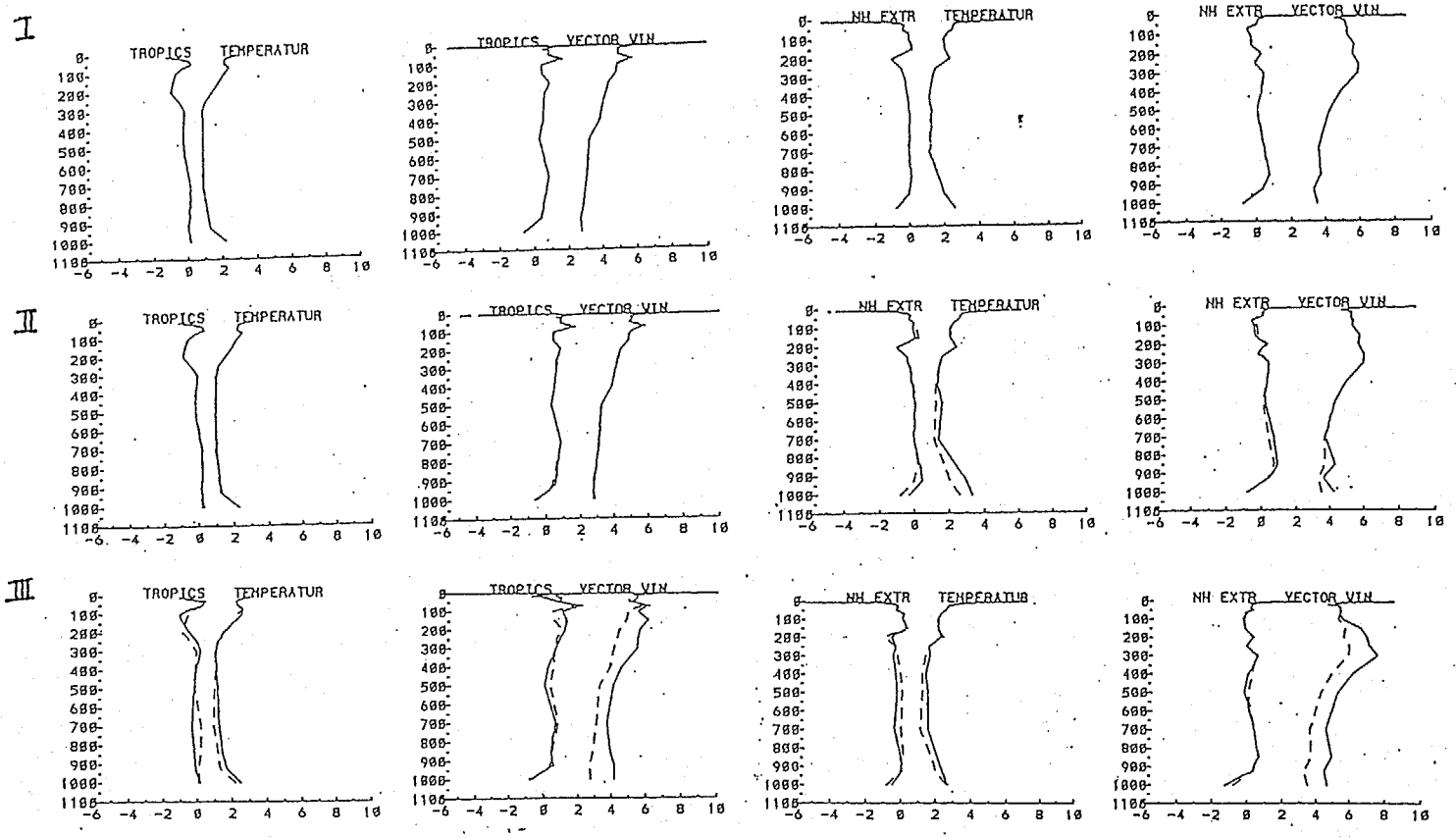
I
TROPICS TEMPERATUR
TROPICS VECTOR VIN
NH EXTR TEMPERATUR
NH EXTR VECTOR VIN
II
TROPICS TEMPERATUR
TROPICS VECTOR VIN
NH EXTR TEMPERATUR
NH EXTR VECTOR VIN
III
TROPICS TEMPERATUR
TROPICS VECTOR VIN
NH EXTR TEMPERATUR
NH EXTR VECTOR VIN

Fig. 9a

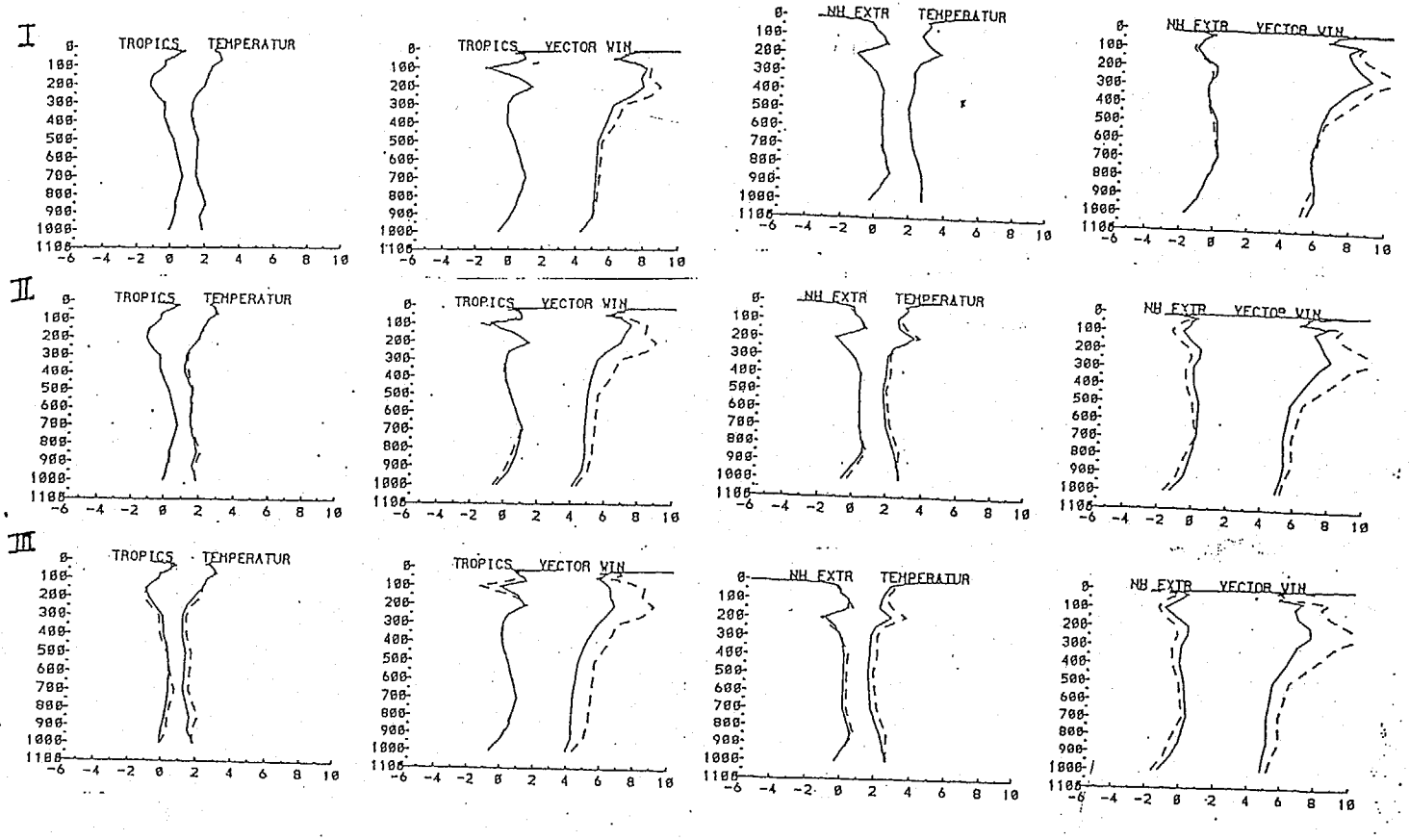
I
TROPICS TEMPERATUR
TROPICS VECTOR WIN
NH EXTR TEMPERATUR
NH EXTR VECTOR WIN
II
TROPICS TEMPERATUR
TROPICS VECTOR WIN
NH EXTR TEMPERATUR
NH EXTR VECTOR WIN
III
TROPICS TEMPERATUR
TROPICS VECTOR WIN
NH EXTR TEMPERATUR
NH EXTR VECTOR WIN

Fig. 9b

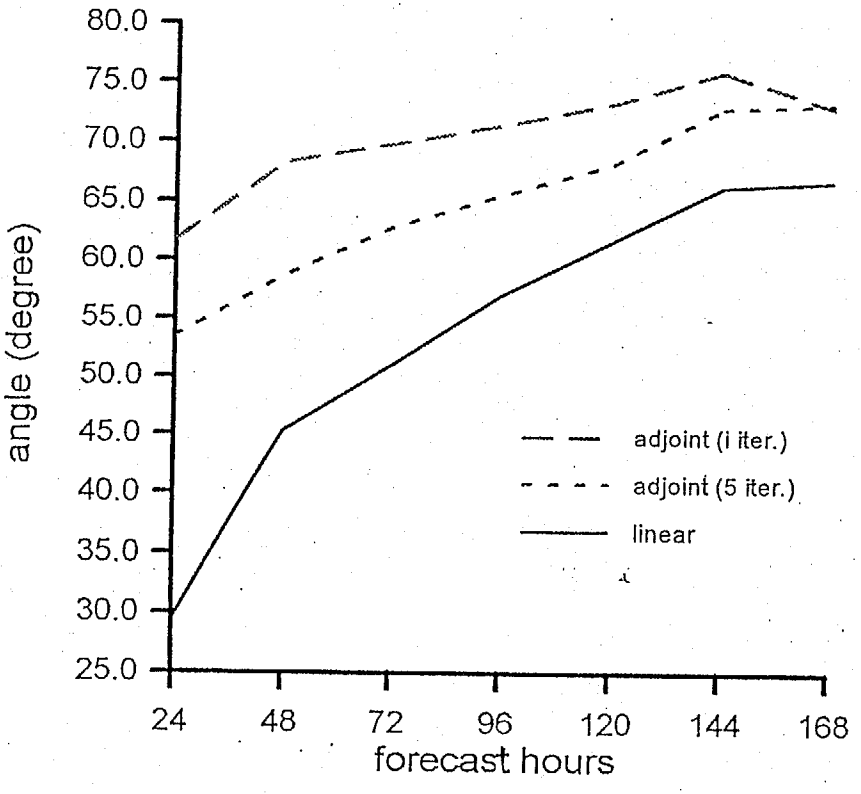
80.0
75.0
70.0
65.0
60.0
55.0
50.0
45.0
40.0
35.0
30.0
25.0
angle (degree)
24
48
72
96
120
144
168
forecast hours
adjoint (i iter.)
adjoint (5 iter.)
linear

Fig. 10

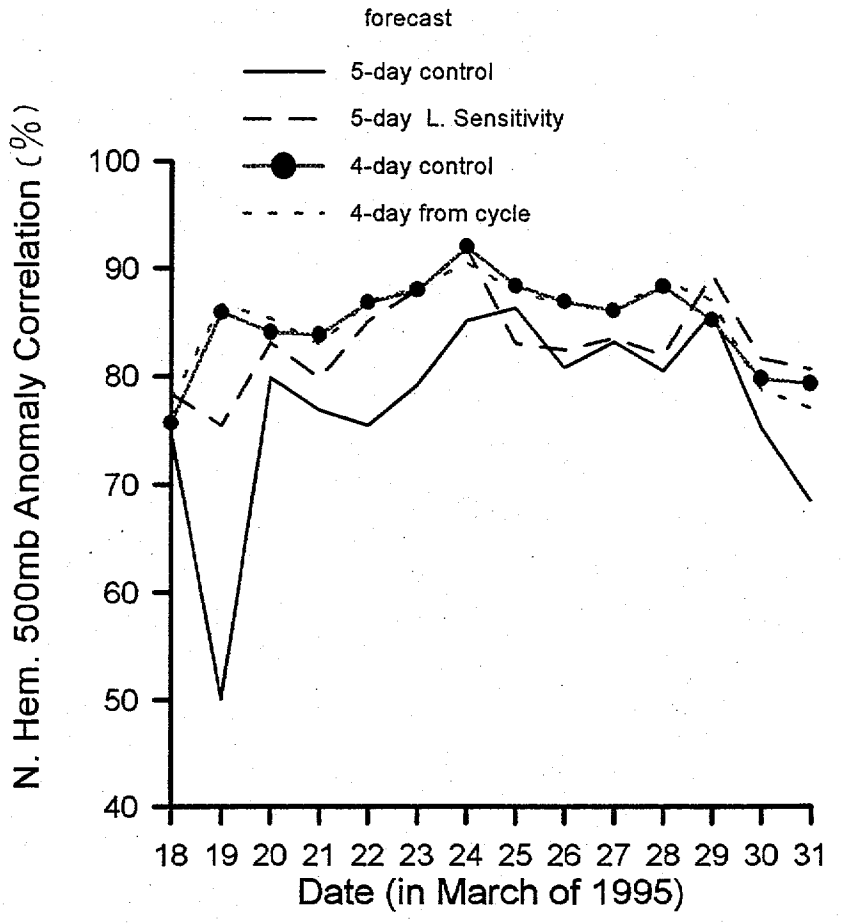
forecast
5-day control
5-day L. Sensitivity
4-day control
4-day from cycle
N. Hem. 500mb Anomaly Correlation (%)
100
90
80
70
60
50
40
18 19 20 21 22 23 24 25 26 27 28 29 30 31
Date (in March of 1995)

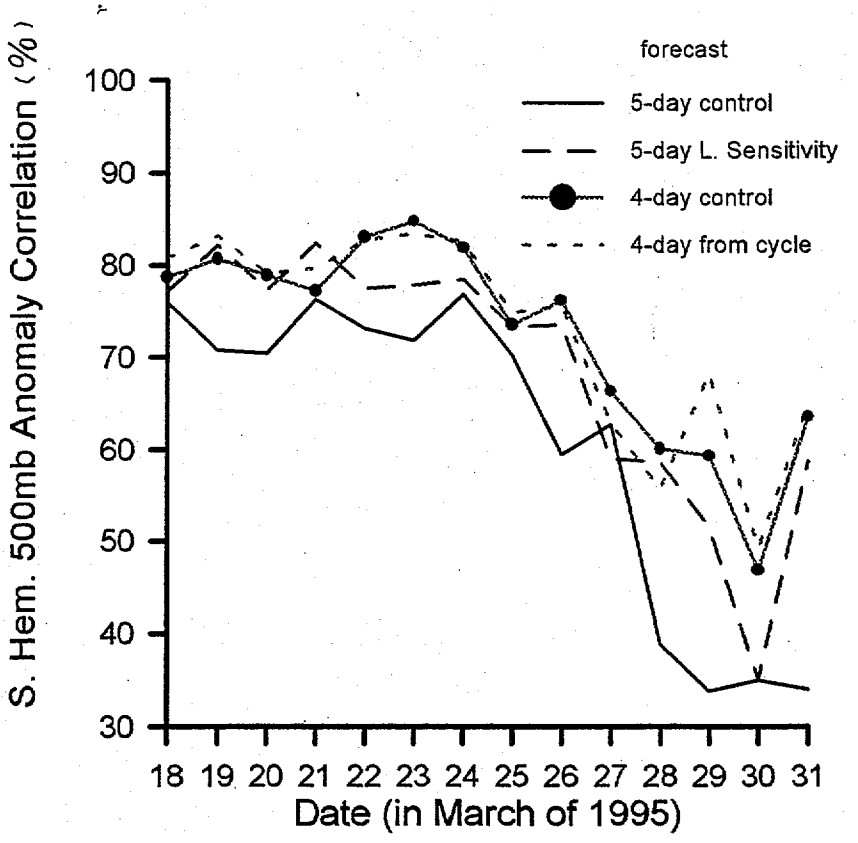
forecast
5-day control
5-day L. Sensitivity
4-day control
4-day from cycle
S. Hem. 500mb Anomaly Correlation (%)
100
90
80
70
60
50
40
30
18 19 20 21 22 23 24 25 26 27 28 29 30 31
Date (in March of 1995)

Fig. 11

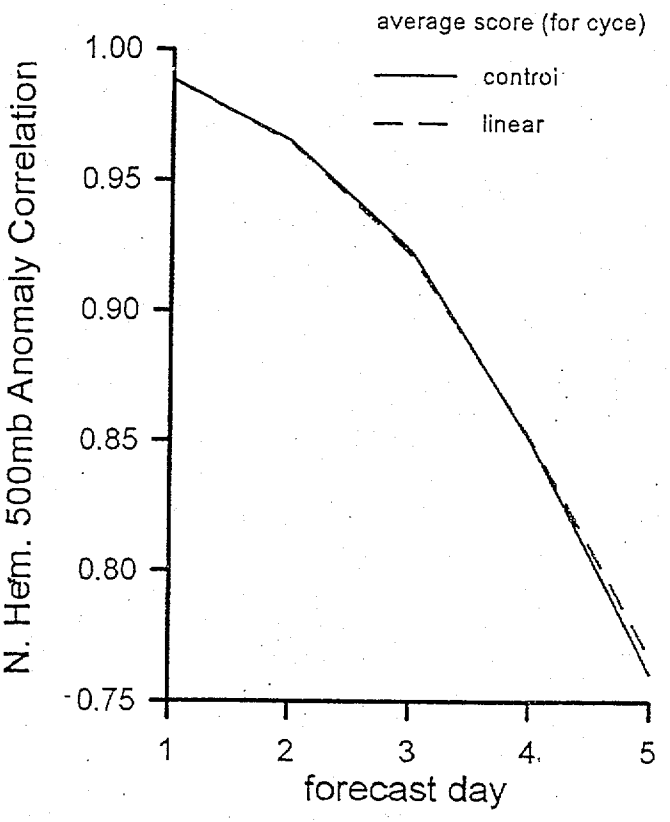
average score (for cyce)
controi
linear
1.00
0.95
0.90
0.85
0.80
0.75
N. Hem. 500mb Anomaly Correlation
1
2
3
4
5
forecast day

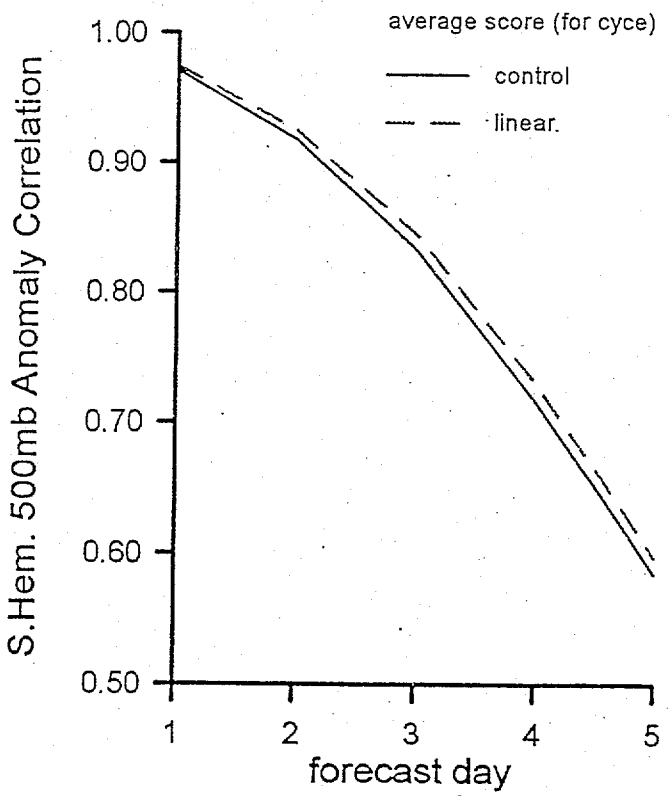
average score (for cyce)
control
linear.
1.00
0.90
0.80
0.70
0.60
0.50
S.Hem. 500mb Anomaly Correlation
1
2
3
4
5
forecast day

Fig. 12

Table. 1 Comparison of The Forecast Anomaly Correlation Scores for Geopotential Height Field (1-20 waves, from 0000UTC 24 March 1995)

	Northern Hemisphere 500mb				Southern Hemisphere 500mb			
Day	Control	Adjoint 1 iter.	Adjoint 5 iter.	TLM	Control	Adjoint 1 iter.	Adjoint 5 iter.	TLM
1	0.9887	0.9933	0.9953	0.9964	0.9804	0.9884	0.9903	0.9953
2	0.9649	0.9724	0.9823	0.9831	0.9516	0.9595	0.9712	0.9702
3	0.9286	0.9462	0.9656	0.9776	0.9119	0.9316	0.9413	0.9348
4	0.8800	0.9058	0.9449	0.9559	0.8471	0.8687	0.8960	0.8820
5	0.8520	0.8437	0.8988	0.8998	0.7691	0.7514	0.7860	0.7980